U.PORTO
FACULDADE DE FARMÁCIA
UNIVERSIDADE DO PORTO

Laboratório de Química Orgânica e Farmacêutica
FACULDADE DE FARMÁCIA U.PORTO

Synthesis of siderophores to produce new antimicrobial adjuvants

Joana Maria André Teixeira

Project I

2022/2023

Synthesis of siderophores to produce new antimicrobial adjuvants

Supervisor: Professora Doutora Emília Sousa

Co-supervisors: Doutora Diana Resende, Mestre Joana Cardoso

Laboratory of Organic and Pharmaceutical Chemistry

Faculty of Pharmacy of University of Porto

Acknowledgments

I would like to acknowledge those who supported me and made this project possible.

I'm deeply grateful to my supervisor Professor Dr. Emília Sousa for the vote of confidence and motivation that allowed me to explore this area of research. Thank you for the guidance and for all the transmitted knowledge.

Additionally, I address my gratitude to my co-supervisor Dr. Diana Resende for always being available to clarify my doubts and for her encouraging words. Her experience was fundamental for this project.

A very especial thank to my co-supervisor MSc Joana Cardoso who was my great support in the laboratory. Thank you for all your availability and kindness in the realization of this project.

I also want to thank all members of the Laboratory of Organic and Pharmaceutical Chemistry for their help and knowledge sharing.

Finally, I'm grateful to my family and friends, who supported me and for their trust and patience.

This research was supported by national funds through FCT - Foundation for Science and Technology within the scope of UIDB/04423/2020, UIDP/04423/2020 (Group of Marine Natural Products and Medicinal Chemistry, CIIMAR), projects EXPL/CTA-AMB/0810/2021, and by the Norte Portugal Regional Operational Programme (NORTE 2020), under the PORTUGAL 2020 Partnership Agreement and through the ERDF, as a result of the project ATLANTIDA (reference NORTE-01-0145-FEDER-000040).

Part of this work was presented in IJUP23 by a poster communication.

Teixeira, J.; Cardoso, J.; Sousa, E.; Resende, D. "Initial steps into the synthesis of a catecholamide siderophore mimetic" IJUP, 13th Edition, Faculty of Pharmacy of University of Porto, 10-12 May **2020**

Index

Acknowledgments ii
Index iii
Index of Figures iv
Index of Tables v
Index of Schemes v
Abstract vi
Resumo vii
Abbreviations and Acronyms: viii
1. Introduction 1
1.1. The problem of antimicrobial resistance 1
1.2. Siderophores 1
1.3. Siderophores-antimicrobials conjugates 3
1.3.1. Natural siderophores-antimicrobial conjugates 4
1.3.2. Synthetic siderophore-antimicrobial conjugates 4
2. Aims 6
3. Results and Discussion 7
3.1. Synthesis of siderophore mimetics 7
3.1.1. Synthesis of 4-(2,3-bis(benzyloxy)benzamide) butanoic acid (1) 7
3.1.2. Synthesis of *N,N'*-(azanediylbis(ethane-2,1-diyl))bis(2,3 bis(benzyloxy)benzamide) (**2**) 7
3.2. Synthesis of Thioxanthones Derivatives 8
3.2.1. Synthesis of 1-chloro-4-hydroxy-9*H*-thioxanthen-9-one (**3**) 8
3.2.2. Synthesis of methyl 2-((1-chloro-9-oxo-9*H*-thioxanthen-4-yl)oxy)acetate (**4**) 9
3.2.3. Synthesis of 2-((1-chloro-9-oxo-9*H*-thioxanthen-4-yl)oxy)acetic acid (**5**) 9
3.2.4. Synthesis of 1-[2-(diethylamino)ethyl]-amino-4-propoxy-9*H*-thioxanthen-9-one (**6**) . 10
3.3. Structure elucidation 11
3.3.1. IR spectroscopy 11
3.3.2. ^{1}H NMR – Proton nuclear magnetic resonance 12
3.3.3. ^{13}C NMR – Carbon Nuclear Magnetic Resonance 13
4. Materials and Methods 15
4.1. Chemistry 15
4.2. Synthesis of siderophore mimetics 15
4.2.1. Synthesis of 4-(2,3-bis(benzyloxy)benzamide)butanoic acid (**1**) 15
4.2.2. Synthesis of *N,N'*-(azanediylbis(ethane-2,1-diyl))bis(2,3-bis(benzyloxy)benzamide (**2**) 16

4.3. Synthesis of thioxanthone derivatives 17
4.3.1. Synthesis of the 1-chloro-4-hydroxy-9*H*-thioxanthen-9-one (**3**) 17
4.3.2. Synthesis of methyl 2-((1-chloro-9-oxo-9*H*-thioxanthen-4-yl)oxy)acetate (**4**)..... 17
4.3.3. Synthesis of 2-((1-chloro-9-oxo-9*H*-thioxanthen-4-yl)oxy)acetic acid (**5**)..... 18
4.3.4. Synthesis of 1-[2-(diethylamino)ethyl]-amino-4-propoxy-9*H*-thioxanthen-9-one (**6**) . 18
5. Conclusion and Future Perspectives: 19
6. References: 20
7. Supporting Information 22

Index of Figures

Figure 1 - Iron-chelated siderophore. 1
Figure 2 - Hexadentate structure of siderophores. 2
Figure 3 - Types of siderophores and examples. 2
Figure 4 - Scheme of siderophore uptake by Gram-negative (left) and Gram-positive bacteria (right) 3
Figure 5 – Cediderocol. 4
Figure 6 - Sideromycins and microcins 4
Figure 7 - Synthetics Siderophores – Antimicrobial Conjugates (A e B). 5
Figure 8 - 1-[2-(Diethylamino)ethyl]-amino-4-propoxy-9H-thioxanthen-9-one (**TxA1**). 6
Figure 9 - 4-(2,3-bis(benzyloxy)benzamide)butanoic acid (**1**), N,N'-(azanediylbis(ethane-2,1-diyl))bis(2,3-bis(benzyloxy)benzamide (**2**), 2-((1-chloro-9-oxo-9H-thioxanthen-4-yl)oxy)acetic acid (**3**) and 1-[2-(diethylamino)ethyl]-amino-4-propoxy-9H-thioxanthen-9-one (**4**) 6
Figure 10 - Structure of 4-(2,3-bis(benzyloxy)benzamide)butanoic acid (**1**), with the respective numbering. ..... **Erro! Marcador não definido.**
Figure 11 - Structure of N,N'-(azanediylbis(ethane-2,1-diyl))bis(2,3-bis(benzyloxy)benzamide (**2**), with the respective numbering. 16
Figure 12 - Structure of 1-chloro-4-hydroxy-9H-thioxanthen-9-one (**3**), with the respective numbering. 17
Figure 13 - Structure of methyl 2-((1-chloro-9-oxo-9H-thioxanthen-4-yl)oxy)acetate (**4**), with the respective numbering 17
Figure 14 - Structure of 2-((1-chloro-9-oxo-9H-thioxanthen-4-yl)oxy)acetic acid (**5**), with the respective numbering 18
Figure 15 - ^{1}H NMR spectrum of compound **1** ($CDCl_3$, 300.13 MHz). 22
Figure 16 - ^{1}H NMR spectrum of compound **2** ($CDCl_3$, 400 MHz). 22
Figure 17 - ^{1}H NMR spectrum of compound **3** (DMSO-d_6, 300 MHz). 23
Figure 18 - ^{1}H NMR spectrum of compound **4** (DMSO-d_6, 400 MHz). 23
Figure 19 - ^{1}H NMR spectrum of compound **5** (DMSO-d_6, 400 MHz). 24
Figure 20 - ^{13}C NMR spectrum of compound **1** (CDCl3, 400 MHz). 24
Figure 21 - ^{13}C NMR spectrum of compound **2** (CDCl3, 400 MHz). 25
Figure 22 - ^{13}C NMR spectrum of compound **4** (DMSO-d_6, 75.45 MHz). 25
Figure 23 - ^{13}C NMR spectrum of compound **5** (DMSO-d_6, 75.45 MHz). 26

Index of Tables

Table 1 - Siderophore applications. 3
Table 2 - IR data for compound **1** and **2**. 11
Table 3 - IR data for compound **3** and **4**. 11
Table 4 - Chemical shifts (δ_H, ppm), multiplicity and coupling constants (J, Hz) of the ^{1}H NMR spectra of compound **1** and **2**. 12
Table 5 - Chemical shifts (δ_H, ppm), multiplicity and coupling constants (J, Hz) of the ^{1}H NMR spectra of compound **3**, **4** and **5**. 13
Table 6 - Chemical shifts (δ_C, ppm) of the ^{13}C NMR spectra of compound **1** and **2**. 13
Table 7 - Chemical shifts (δ, ppm) of the ^{13}C NMR spectra of compounds **4** and **5**. 14

Index of Schemes

Scheme 1 - Synthesis of 4-(2,3-bis(benzyloxy)benzamide) butanoic acid (**1**). 7
Scheme 2 - Synthesis of N, N'-(azanediylbis(ethane-2,1-diyl))bis(2,3- bis(benzyloxy)benzamide) (**2**) .. 8
Scheme 3 - Synthesis of 1-chloro-4-hydroxy-9H-thioxanthen-9-one (**3**). 8
Scheme 4 - Synthesis of methyl 2-((1-chloro-9-oxo-9H-thioxanthen-4-yl)oxy)acetate (**4**). 9
Scheme 5 - Synthesis of 2-((1-chloro-9-oxo-9H-thioxanthen-4-yl)oxy)acetic acid (**5**). 9
Scheme 6 - Synthesis of 1-[2-(diethylamino)ethyl]-amino-4-propoxy-9H-thioxanthen-9-one (**6**). 10

Abstract

Siderophores are small molecules of low molecular weight with great affinity to chelate ferric iron [Fe(III)] and other metals. They are of natural origin, with great structural variety. The most common structures of siderophores belong to the groups of catechols, hydroxamates and carboxylates. Currently, research investigations are based on these complex structures to develop mimetics, with several applications, namely, to combine with antimicrobials, thus increasing their activity.

Cefiderocol (Fecroja® or Fetcroja®) was the first siderophore-antimicrobial conjugate to be approved by the Food and Drug Administration (FDA) and European Medicines Agency (EMA) to combat urinary tract infections. This conjugate acts as a Trojan Horse, masking the entry of the antimicrobial through the siderophore transport system. Synthetic conjugates usually contain a linker that joins the siderophore to the antimicrobial and it may or may not be cleavable. These conjugates have been the subject of major investigation since they can become a new strategy against antimicrobial resistance.

In this project, the synthesis of two potentials catecholamide siderophores mimetics (compounds **1** and **2**) was carried out, through coupling reactions of 2,3-bis(benzyloxy)benzoic acid with primary amines (γ-aminobutyric acid and diethylenetriamine, respectively).

Furthermore, an aminothioxanthone with antimicrobial activity (**6**) was synthesized and modified, in order to, in the future, proceed to its conjugation with *N,N'*-(azanediylbis(ethane-2,1-diyl))bis(2,3-bis(benzyloxy)benzamide) (**2**). A sequence of four syntheses was carried out until the desired aminothioxanthone (**6**) was obtained. The first three steps consisted of the formation of 2-((1-chloro-9-oxo-9*H*-tioxanthen-4-yl)oxy)acetic acid (**5**), which corresponds to a thioxanthone derivative associated with the linker. The last reaction consisted of the addition of *N,N*-diethylethane-1,2-diamine to form 1-[2-(diethylamino)ethyl]-amino-4-propoxy-9*H*-thioxanthen-9-one(**6**).

Synthetic details and structural characterization (by infrared and nuclear magnetic resonance spectroscopy) of the synthesized compounds were presented and discussed.

In conclusion, the synthesis of the six compounds were achieved. In the future, the following step is the conjugation of the *N,N'*-(azanediylbis(ethane-2,1-diyl))bis(2,3-bis(benzyloxy)benzamide) (**2**) with the synthesized aminothioxanthone (**6**) in order to obtain the siderophore-antimicrobial conjugate with a potential activity against resistance to antimicrobials, which must be confirmed.

Resumo

Os sideróforos são pequenas moléculas de baixo peso molecular com grande afinidade para quelatar o ferro férrico [Fe(III)] e outros metais. São moléculas de origem natural, com grande variedade estrutural. As estruturas mais comuns usadas como adjuvantes de antimicrobianos pertencem aos grupos dos catecóis, hidroxamatos e carboxilatos. Atualmente, os investigadores baseiam-se nestas estruturas complexas para desenvolver miméticos, com diversas aplicabilidades, nomeadamente conjugar com antimicrobianos, aumentando a atividade destes.

O cefiderocol (Fecroja® ou Fetcroja®) foi o primeiro conjugado sideróforo-antimicrobiano a ser aprovado pela FDA e EMA, para combater infeções do trato urinário. Estes conjugados atuam como Cavalos de Troia, mascarando a entrada do antimicrobiano através do sistema de transporte de sideróforos. Os conjugados sintéticos contêm um linker que une o sideróforo ao antimicrobiano e que pode ser ou não clivável. Estes têm sido alvo de grande investigação, uma vez que podem vir a ser uma nova estratégia contra a resistência a antimicrobianos.

Neste projeto foi realizada a síntese de dois potenciais miméticos de sideróforos de catecolamidas (compostos **1** e **2**), através de reações de acoplamento do ácido 2,3-bis(benziloxi)benzoico com aminas primárias (ácido γ-aminobutírico e dietilenetriamina, respetivamente).

Além disso procedeu-se à síntese de uma aminotioxantona, com potencial atividade antimicrobiana, para que no futuro seja possível conjuga-lo com o *N,N'*-(azanediilbis(etano-2,1-diil))bis(2,3-bis(benziloxi)benzamida) (**2**). Para isso, realizou-se uma sequência de quatro sínteses até se obter a aminotioxantona desejada. As primeiras três etapas consistem na formação do ácido 2-((1-cloro-9-oxo-9*H*-tioxanten-4-il)oxi)acético (**5**), que corresponde um derivado de tioxantona associado ao "linker". A última reação consiste na adição da *N*,*N*-dietiletano-1,2-diamina para a formação da 1-[2-(dietilamino)etil]-amino-4-propoxi-9*H*-tioxanten-9-ona (**6)**.

Os detalhes sintéticos e a caracterização estrutural (espetrometria de infravermelho e ressonância magnética nuclear) dos compostos sintetizados foram apresentados e discutidos.

Em conclusão, a síntese dos seis compostos foi conseguida. O passo seguinte será a conjugação do *N,N'*-(azanediilbis(etano-2,1-diil))bis(2,3-bis(benziloxi)benzamida) (**2**) com a aminotioxantona (**6**), de forma a obter o conjugado sideróforo-antimicrobiano, com potencial atividade contra a resistência a antimicrobianos, a qual tem de ser confirmada.

Abbreviations, Acronyms and Symbols

ATP – Adenosine triphosphate

^{13}C NMR – Carbon Nuclear Magnetic Resonance

^{1}H NMR – Proton Nuclear Magnetic Resonance

d – Duplet

DCC – *N,N'*-Dicyclohexylcarbodiimide

dd – Double duplet

ddd – Doudle double duplet

dt – Double triplet

EMA – European Medicines Agency

FDA – Food and Drug Administration

HSQC – Heteronuclear Single Quantum Coherence

HMBC – Heteronuclear Multiple Bond Correlation

Hz – Hertz

IR - Infrared

J – Coupling constant

m – Multiplet

MDR – Multi-drug resistance

MeOH – Methanol

MHz – MegaHertz

MIC – Minimum inhibitory concentration

NHS – *N*-Hydroxysuccinimide

NMR – Nuclear Magnetic Resonance

p – Quintet

ppm - parts per million

q – Quartet

s – Singulet

SBPs – Lipoprotein siderophore-binding proteins

t – Triplet

TBDT – TonB-dependent transport

THF – Tetrahydrofuran

δ – Chemical shift

CDI – 1,1' -Carbonyldiimidazole

DMSO-d_6 – Dimethyl sulphoxide-d6

UV – Ultraviolet

TLC – Thin layer chromatography

1. Introduction

1.1. The problem of antimicrobial resistance

The issue of antimicrobial resistance has become a growing concern in society in recent years. Unfortunately, the discovery of new antimicrobials has not kept pace with this increase, making it even more challenging to address this significant public health problem.
The reducing of activity of numerous compounds due to multi-drug resistance (MDR) can have a significant impact on the treatment of various microbiological infections and other pathologies such as cancer[1]. One of the most common strategies of resistance to chemotherapy is to reduce the drugs' ability to reach therapeutic concentrations inside the microorganism. Modifications in the structures responsible for drug entry and the increased number of efflux pumps pose a challenge to antimicrobial action, resulting in only subtoxic concentrations remaining inside the cells[2].
In addition to the discovery of new antimicrobials, researchers have also explored alternative solutions to the problem of resistance over the past few decades. One such approach involves siderophore conjugates, which act as Trojan horses and facilitate the entry of antimicrobials into the cell.

1.2. Siderophores

Iron is one of the most abundant elements in the Earth's crust[3]. It plays a vital role in the e growth and survival of microorganisms and plants as it facilitates crucial metabolic processes including enzymatic processes, oxygen metabolism, electron transfer, and DNA and RNA synthesis. Additionally, it's also important for biofilm formation[4]. Despite its importance, its low solubility limits its bioability in aerobic environments[5]. Microorganisms have developed strategies to overcome this adversity and obtain iron from soil and water. One effective strategy is the production and secretion of siderophores, compounds synthesized by microorganisms such as bacteria and fungi in iron-poor conditions. Siderophores are capable of capturing the insoluble Fe(III) and making accessible for absorption[2]. The word siderophore is derived from the Greek "sidero" + "phore" which means iron + bearer[2]. These low-molecular iron chelators have more affinity for Fe(III) than for Fe(II) (Figure 1). Nonetheless, they can complex other elements such as Mn^{3+}, Co^{3+}, and Ni^{2+}. To date, more than 500 siderophore structures have been elucidated[4].

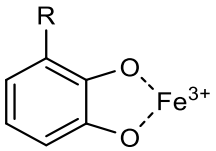

Figure 1 - Iron-chelated siderophore.

Siderophores are negatively charged molecules by oxygen atoms, that establish strong bonds with Fe(III). However, they can have other atoms like nitrogen and sulfur with less affinity to iron[3]. For the binding of siderophores with the central Fe(III), with minimal repulsion between the ligands, they organize into a hexadentate structure with an octahedral geometry (Figure 2) [5].

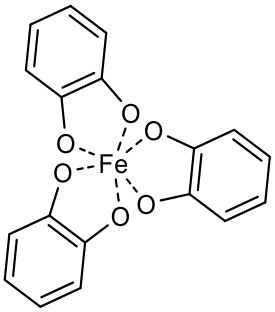

Figure 2 - Hexadentate structure of siderophores.

The most common microbial siderophores are bidentate ligands[5] can be classified in three different groups[2, 4] —catecholates, hydroxamates, and α-hydroxycarboxylates—according to the chemical nature of their coordination site with iron. Additional, siderophores bearing a mixture of these were also identified (Figure 3). Even though all these groups are abundant in nature, the catecholates possesses a highest affinity for iron as a result of the *ortho*-phenolate[5].

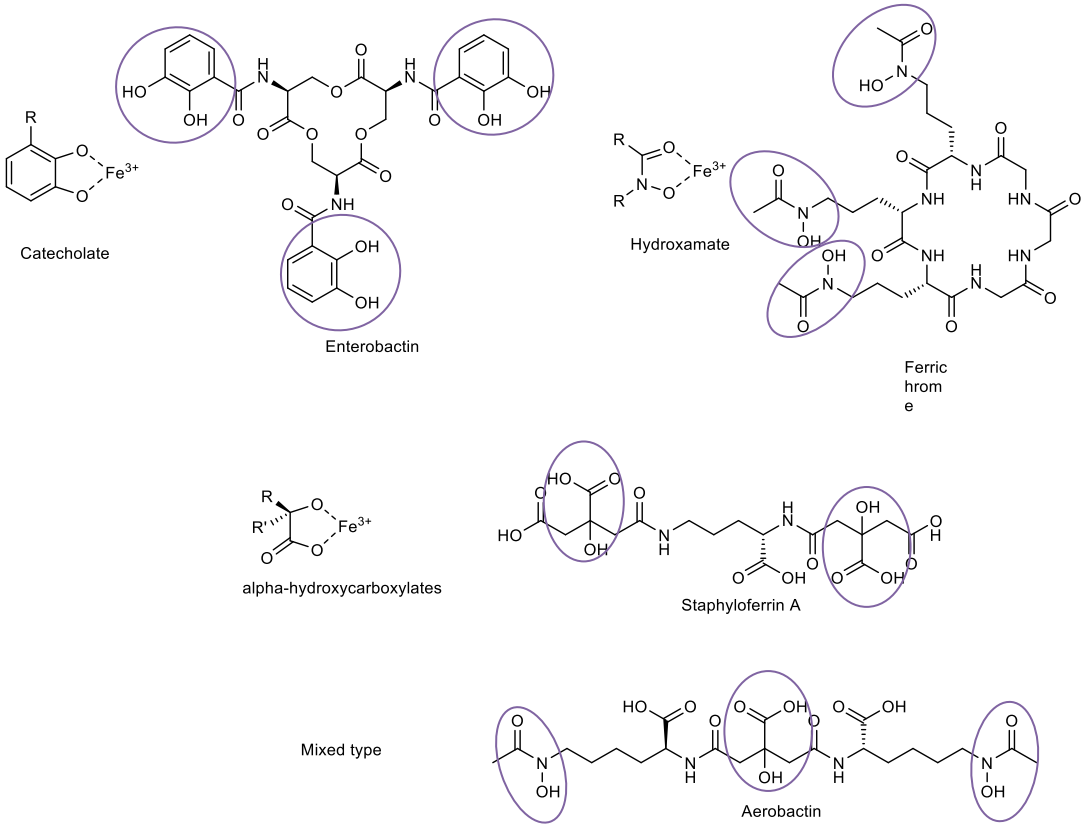

Figure 3 - Types of siderophores and examples.

Microorganisms have a specific mechanism for the uptake of the iron-siderophore complex. In bacteria, this differs if they are Gram-negative or Gram-positive. In Gram-negative bacteria, the iron-siderophore complex is recognized by TonB-dependent receptors and transported to the outer membrane through TonB-dependent transport (TBDT). When the complex reaches the periplasm, the complex passes the cell wall through lipoprotein siderophore-binding proteins (SBPs). After that, it crosses the membrane into the cytoplasm by ATP-binding cassettes (ABC) transport system. Both transport systems are energy-dependent (Figure 4)[2].

In Gram-positive bacteria, even though the transport also requires spending ATP, they don't need the TBDT transport. The iron-siderophore complex crosses the cell wall by SBPs anchored to the

membrane. This system is the same that Gram-negative bacteria uses[4]. The SBP system has a permease and an ATPase that import the complexes into the cytoplasm (Figure 4)[2].
Once the complex is inside the cell, the iron is released from the siderophore carrier due to a loss of stability of the iron-siderophore complex, which leads to a reduction of the Fe(III) and the respective separation[4]. This cleavage may also occur from a hydrolytic mechanism depending on the siderophore structure[2].

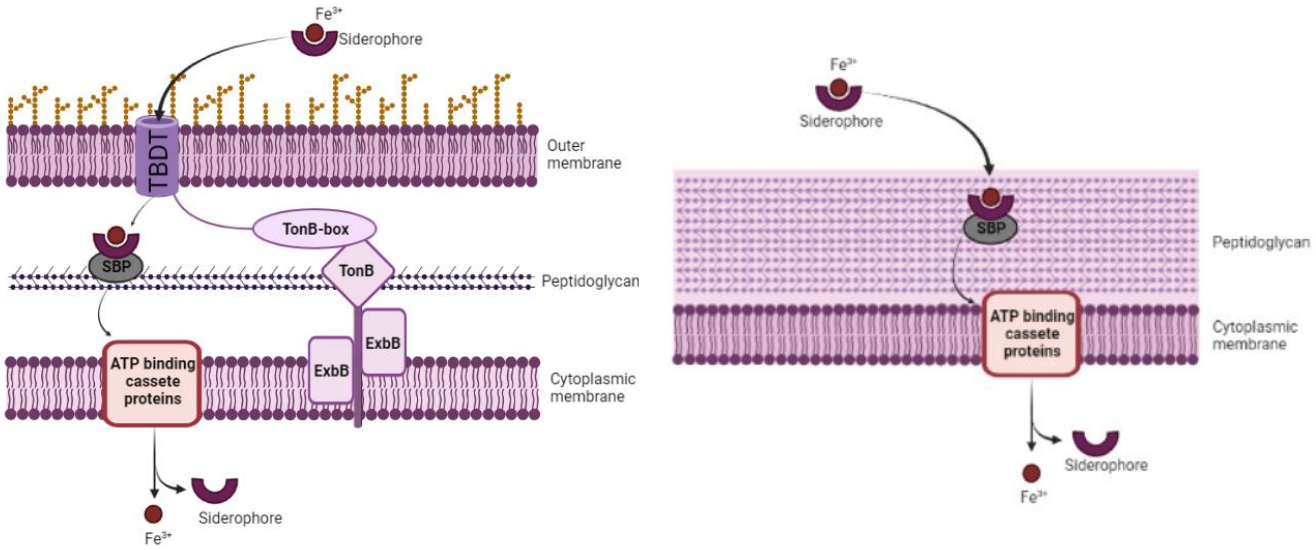

Figure 4 - Scheme of siderophore uptake by Gram-negative (left) and Gram-positive bacteria (right) (Adapted from Almeida *et al.*[1] and created with BioRender.com).

Considering the importance of siderophores for microorganism survival, they're the target of many studies and Table 1 presents some described applications that have been investigated over the last years.

Table 1 - Siderophore applications.

Medical Applications	Nature Applications	Biotechnological applications
Iron-chelated therapy[3]	Soil mineral weathering[3]	Promotion of plant growth[3]
Antimicrobial conjugates[1]	Biogeochemical cycling of Fe in the ocean[3]	Biocontrol of fish pathogens[4]
Anticancer conjugates[1]		Microbial ecology and taxonomy[4]
Metalloenzymes inhibitors[3]		Bioremediation of environmental pollutants [4]
Diagnostic techniques[1]		Soil bioremediation[3]
		Nuclear fuel reprocessing[4]
		Optical biosensor[4]

1.3. Siderophores-antimicrobials conjugates

Recently, the novel siderophore-antimicrobial conjugate, cefiderocol (Figure 5) was approved by FDA (Fetroja®, 2019) and EMA (Fetcroja®, 2020), for urinary tract infections[6]. It's a cephalosporin associated with a catechol siderophore mimetic having antimicrobial activity against Gram-negative bacteria[7], acting as a Trojan horse. This approach allows the conjugate to hijack the bacteria transport system[1], improving the uptake of the antimicrobial and consequently reducing the minimal inhibitory

concentration (MIC)[3]. Furthermore, during the infections there is an increased need for iron by the bacteria, once this element is limited, leading to an increasing need for siderophores. Therefore, this environment is favorable for the best uptake of the antimicrobial[1, 4].

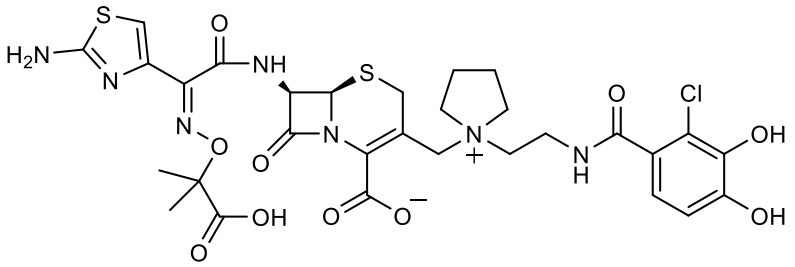

Figure 5 – Cediderocol.

1.3.1. Natural siderophores-antimicrobial conjugates

The most common natural conjugates are produced by Gram-negative bacteria, but some of them are producer by Gram-positive bacteria[1] and other microorganisms. An important group produced by the microorganism *Streptomyces griseoflavus*[5], as a protective strategy against Gram-negative and positive bacteria, are the sideromycins (Figure 6). They are hydroxamates with a typical hexadentate structure linked to the antimicrobial moiety through an amide. Other examples include the microcins (Figure 6) produced by some bacteria that contain a glycosylated siderophore moiety with catechol groups and can act against Gram-positive bacteria[1].

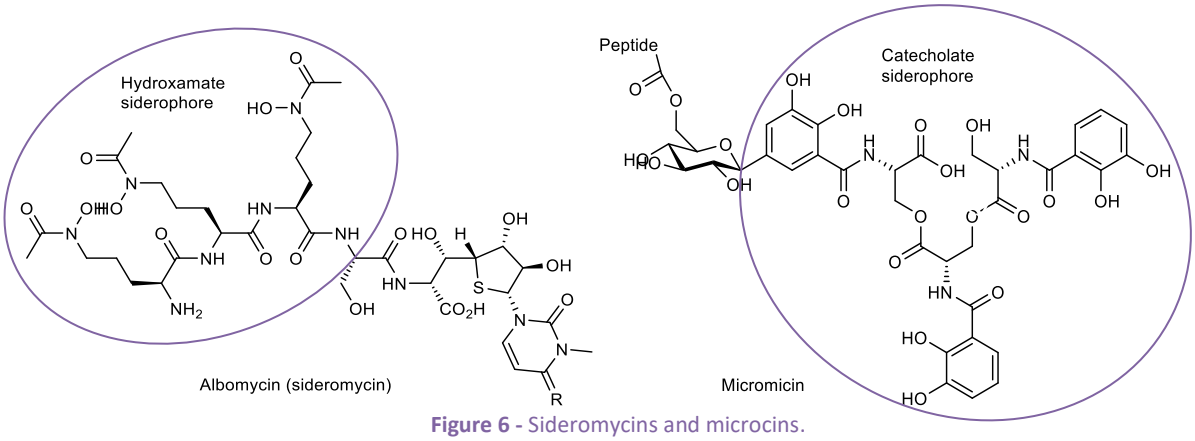

Figure 6 - Sideromycins and microcins.

1.3.2. Synthetic siderophore-antimicrobial conjugates

Researchers were inspired by the natural siderophores to synthesize new siderophores mimetics[1, 3]. These compounds are conjugated with antimicrobial agent to increase the activity and spectrum of action. Although the natural siderophores are more selective, the synthetic mimetics are usually simpler both structurally and in terms of chiral centers and are therefore easier to obtain[1].

The siderophore-antimicrobial conjugates are composed of three parts: the siderophore, as explained above, which allows the complex to enter the cell; the antimicrobial, which will carry out its cytotoxic action inside the cells; and in most cases the linker, whose stability is important to position the two previous molecules at the correct place[1]. The synthetic conjugates can be classified as non-cleavable conjugates and cleavable conjugates, depending on antibiotics' capacity to have or not activity when conjugated.

1.3.2.1. Non-cleavable conjugates

In non-cleavable conjugates, the antimicrobial retains its activity even without the separation from the siderophore. This approach avoids stability problems, very common in the cleavable linker. However, they also present some problems interacting with the antimicrobial target because the siderophore can cause steric hindrance. The non-cleavable conjugates, when used against Gram-negative bacteria, will act in the periplasm or outer membrane once it's very difficult for them to cross into the cytoplasm[1].

1.3.2.2. Cleavable Conjugates

In cleavable conjugates, the release of the siderophore moiety, after crossing the membrane, is a fundamental step for antimicrobial activation, converting these conjugates into prodrugs. The cleavable conjugates are associated with problems affiliated to linker stability. The linker cannot be very unstable and cleave before it reaches the target, but it also cannot be very stable, making it impossible to cleave and release the antimicrobial from the carrier siderophore at the local of action. A way to prevent this is to use a linker that cannot be hydrolyzed, but takes advantage of bacterial enzymes, such as proteases and beta-lactamases, that cleave the linker[1, 3].

After the approval of cefiderocol, the demand for new siderophore-antimicrobial conjugates increased. Many attempts have been developed in this way, and compounds A and B (Figure 7) are examples of it. Compound A, is a non-cleavable conjugate, containing fimbactin, as a siderophore moiety, linked to the antibiotic loracarbet[1]. Compound B was inspired by the natural siderophore sideromycin, desferrioxamine B, which was linked to triclosan through an ester linker[8].

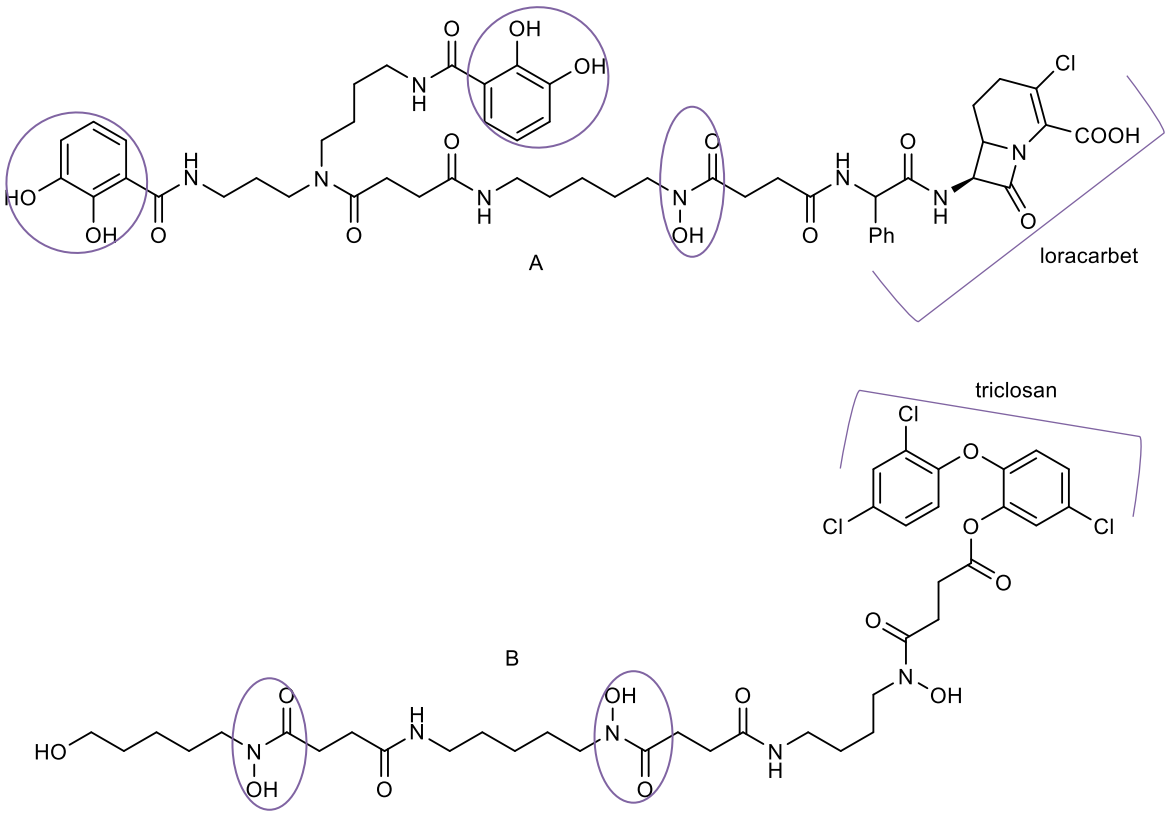

Figure 7 - Synthetics Siderophores – Antimicrobial Conjugates (A e B).

2. Aims

Recent results from our research group have demonstrated that 1-[2-(diethylamino)ethyl]-amino-4-propoxy-9*H*-thioxanthen-9-one (**TxA1**, Figure 8) has a variety of pharmacological activities, such as antibacterial[2, 9], antischistosomals and antitumoral activities[10], and as efflux pump modulator[11].

Based on the mentioned above, the combination of this thioxanthone with a siderophore mimetic(s) was considered to be a suitable starting point for the development of potential new conjugations and the optimization of its antimicrobial activity.

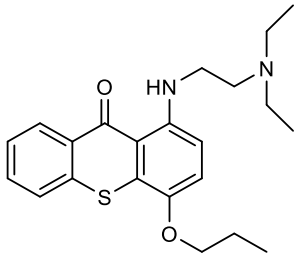

Figure 8 - 1-[2-(Diethylamino)ethyl]-amino-4-propoxy-9*H*-thioxanthen-9-one (**TxA1**).

The aims of this project consist in:
- the synthesis of two potential siderophore mimetics, compound **1** and compound **2**,
- the synthesis of a thioxanthone linked to the linker (**5**) and subsequently addition of an amine to the structure, forming an aminothioxanthone (**6**) and,
- structural elucidation of all compounds obtained by spectroscopic techniques such as ^{1}H and ^{13}C nuclear magnetic resonance.

Ultimately, the main goal is to obtain *N,N'*-(azanediylbis(ethane-2,1-diyl))bis(2,3-bis(benzyloxy)benzamide) (**2**) and aminothioxanthone (**6**) in sufficient amount for further conjugation of both of these compounds.

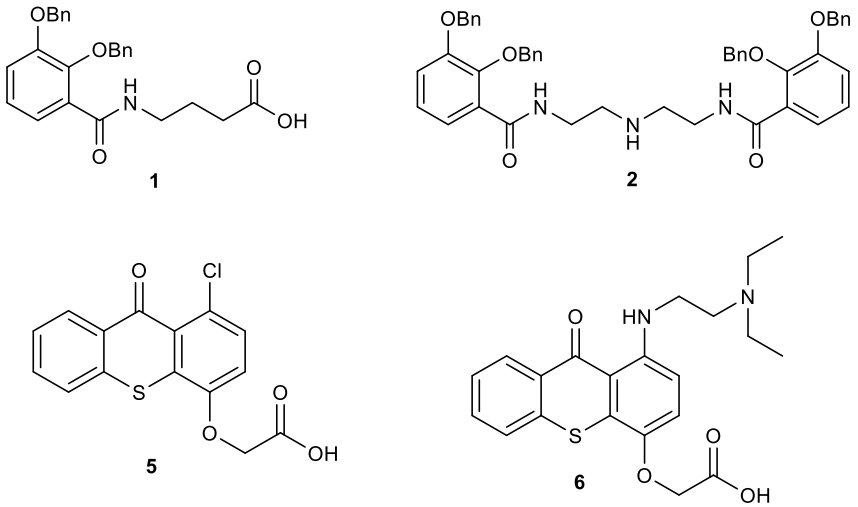

Figure 9 - 4-(2,3-Bis(benzyloxy)benzamide)butanoic acid (**1**), *N,N'*-(azanediylbis(ethane-2,1-diyl))bis(2,3-bis(benzyloxy)benzamide (**2**), 2-((1-chloro-9-oxo-9*H*-thioxanthen-4-yl)oxy)acetic acid (**3**) and 1-[2-(diethylamino)ethyl]-amino-4-propoxy-9*H*-thioxanthen-9-one (**4**).

3. Results and Discussion

3.1. Synthesis of siderophore mimetics

Considering the potential of catechol as a siderophore mimetic, the synthesis and characterization of two catechol molecules will be presented in this work. In order to form the desired products, through the formation of an amide bond, the hydroxyl groups of commercial 2,3-dihydroxybenzoic acid were protected, allowing, the carboxylic acid to be easily functionalised with different *N*-acyl hydroxamate groups, as described[10].

3.1.1. Synthesis of 4-(2,3-bis(benzyloxy)benzamide) butanoic acid (1)

The formation of compound **1** consists of the amide coupling of 2,3-bis(benzyloxy)benzoic acid with commercial γ-aminobutyric acid[9] (Scheme 1). In the first step of this reaction, *N*,*N*'-dicyclohexylcarbodiimide (DCC), a strong activator of carboxylic acid, was used under anhydrous conditions to form an active intermediate of 2,3-bis(benzyloxy)benzoic acid. *N*-hydroxysuccinimide (NHS) was also used to aid the formation of the intermediate, once it bonds to the DDC making it even more efficient, increasing yields[14]. After the 3 hours of stirring in tetrahydrofuran (THF) at room temperature, besides the formation of the intermediate, it also formed *O*-acylurea and dicyclohexylurea. Since these two by-products were insoluble in THF, the precipitate was removed by filtration. The second step of the reaction involves the interaction of γ- aminobutyric acid with the intermediate in the presence of $KHCO_3$, which creates a favourable alkaline environment for the reaction, in a mixture of water and THF (1:1) at room temperature for 24 hours.

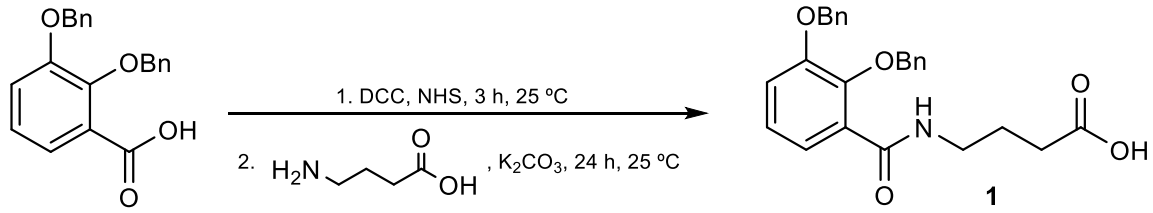

Scheme 1 - Synthesis of 4-(2,3-bis(benzyloxy)benzamide) butanoic acid (**1**).

The evolution of the reaction was followed by TLC using a mixture of CH_2Cl_2:MeOH (9:1)) as mobile phase, and observed under ultraviolet (UV) light at 254 and 365 nm. At the end of the reaction, the THF was removed by evaporation under reduced pressure. The crude was dissolved in citric acid and subjected to multiple liquid-liquid extractions with ethyl acetate to remove compound **1** and other remaining organic molecules. The aqueous phase removed the base and remaining amine. Finally, flash column chromatography was performed to purify and isolate compound **1**, obtaining a 78 % yield.

3.1.2. Synthesis of *N,N'*-(azanediylbis(ethane-2,1-diyl))bis(2,3 bis(benzyloxy)benzamide) (**2**)

For the synthesis of compound **2**, the carboxylate of 2,3-bis(benzyloxy)benzoic acid was coupled with diethylenetriamine, via amide bond formation[10] (Scheme 2).

1,1' -Carbonyldiimidazole (CDI) was added to a 2,3-bis(benzyloxy)benzoic acid solution in dry/anhydrous dichloromethane (CH_2Cl_2) and stirred at room temperature under nitrogen atmosphere for 2 h. This reagent is used frequently to activate carboxylic acids and promote the coupling with amines via imidazolides to form amides. They also present some other advantages

compared to other reagents such as DCC, since the products are easily removed from the reaction mixture[15]. After 2 hours, the N-acyl imidazole intermediate was formed. The second step consisted in the formation of compound 2 through the reaction of the diethylenetriamine, dissolved in dry CH_2Cl_2, with the intermediate, stirred for 14 hours at room temperature.

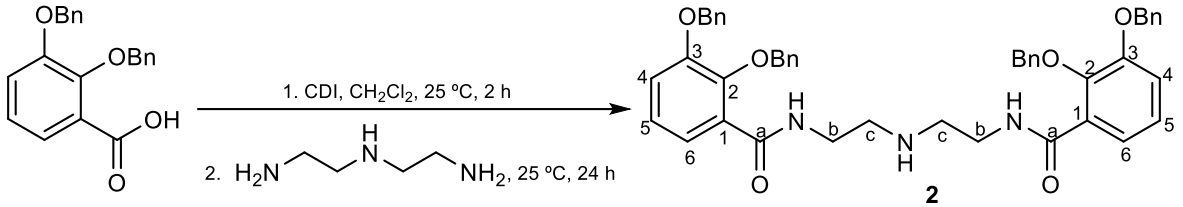

Scheme 2 - Synthesis of *N, N'*-(azanediylbis(ethane-2,1-diyl))bis(2,3- bis(benzyloxy)benzamide) (**2**).

The progression of the reaction was monitored by TLC using a mixture of CH_2Cl_2:MeOH (9:1) as mobile phase and observed under UV light at 254 and 365 nm. When the reaction was completed, the mixture was concentrated and purified by column chromatography, with a 72% yield.

3.2. Synthesis of Thioxanthones Derivatives

In this project, the linker was added to the thioxanthone, instead of the siderophore. The direct conjugation of the linker to the siderophore would lead to a lack of a binding site for thioxanthone, being necessary to create another structural modification.
Cardoso *et al.* demonstrated that a change in the substituent groups at the C-4 position of the thioxanthone scaffold appears not to be crucial for antimicrobial activity[12]. Therefore, it's predictable that with the substitution of the linker, the compound's activity will remain. However, it is necessary to carry out further antimicrobial tests to confirm this hypothesis.

3.2.1. Synthesis of 1-chloro-4-hydroxy-9*H*-thioxanthen-9-one (**3**)

The synthesis of compound **3** consisted of the dealkylation of a commercial chlorinated thioxanthone, dissolved in CH_2Cl_2 (Scheme 3) [12]. Aluminium chloride ($AlCl_3$), a Lewis acid usually used in demethylation reactions, was added in excess[16]. In this case, the conversion of a propoxy group to a hydroxyl group led to the formation of 1-chloro-4-hydroxy-9*H*-thioxanthen-9-one (**3**). The reaction was stirred at 40 °C for 24 hours and its evolution was controlled by TLC using a mixture of *n*-hexane:ethyl acetate (5:5) as mobile phase and observed under UV light at 254 and 365 nm.

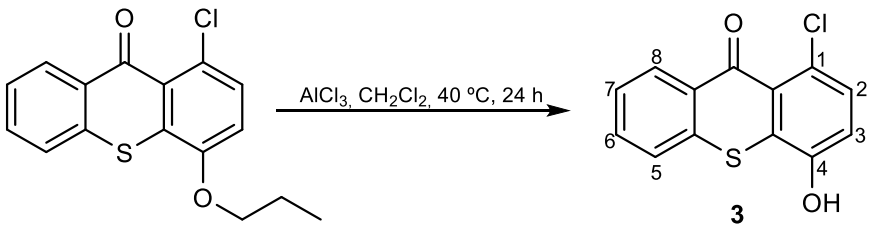

Scheme 3 - Synthesis of 1-chloro-4-hydroxy-9*H*-thioxanthen-9-one (**3**).

After reaction completion, a wash with NaOH was performed, to remove the excess of demethylation agent, and HCl, to deionize the compound **3**, which returns to the organic phase. Then, the organic layer was dried with Na_2SO_4, to remove water residues, filtered, and evaporated under reduced pressure. The concentrate rendered 1.1 g of compound **3**(87 % yield).

3.2.2. Synthesis of methyl 2-((1-chloro-9-oxo-9*H*-thioxanthen-4-yl)oxy)acetate (**4**)

Compound **4** is synthesized by a Williamson ether synthesis, using an alkyl halide containing an ester group, methyl bromoacetate (Scheme 4) [13, 17]. The hydroxy compound **3** and K_2CO_3 were initially dissolved in anhydrous acetone and then, $BrCH_2COOCH_3$ was added. The base, K_2CO_3, ionized the hydroxyl group of compound **3**, to favour the reaction, which was refluxed and stirred for 24 hours. The evolution of the reaction was monitored by TLC using a mixture of *n*-hexane:ethyl acetate (5:5) as mobile phase and observed under UV light at 254 and 365 nm.

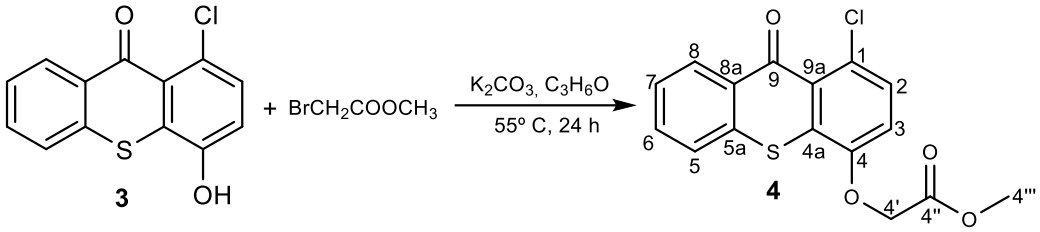

Scheme 4 - Synthesis of methyl 2-((1-chloro-9-oxo-9*H*-thioxanthen-4-yl)oxy)acetate (**4**).

After reaction completion, the mixture was concentrated, and it was performed a multiple liquid-liquid extraction with ethyl acetate to extract the desired compound and a wash with water to remove the excess of base. The organic layer obtained was concentrated and crystallized from MeOH, to eliminate impurities, obtaining compound **4** with a yield of 97 % (61.9 mg).

3.2.3. Synthesis of 2-((1-chloro-9-oxo-9*H*-thioxanthen-4-yl)oxy)acetic acid (**5**)

The synthesis of compound **5** consists of the demethylation of methyl 2-((1-chloro-9-oxo-9*H*-thioxanthen-4-yl)oxy)acetate (**4**), through an alkaline hydrolysis (Scheme 5) [13]. For this, a strong base such as NaOH is added to compound **4** dissolved in CH_2Cl_2/MeOH (1:1, 10 mL), at room temperature, under stirring, forming a salt of compound **5**.

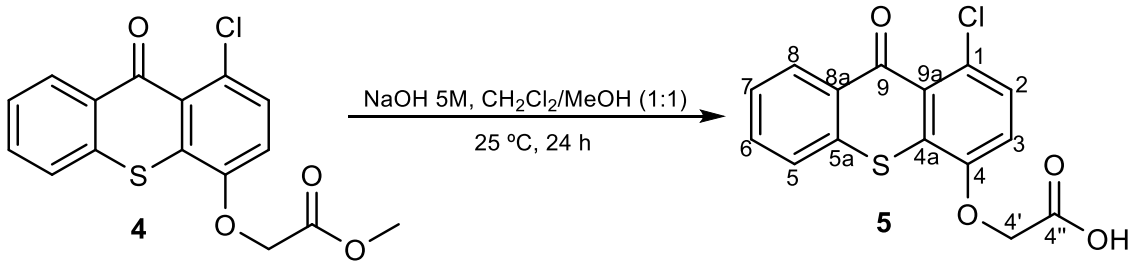

Scheme 5 - Synthesis of 2-((1-chloro-9-oxo-9H-thioxanthen-4-yl)oxy)acetic acid (**5**).

The reaction was monitored by TLC analysis using a mixture of ethyl acetate:*n*-hexane (5:5) as mobile phase and was observed under UV light at 254 and 365 nm. After 24 hours, the reaction was stopped, and the organic solvents were evaporated under reduced pressure. Since the compound formed was in the form of a salt, it was necessary to add HCl, after dissolved in water, to form compound **5**, which precipitates. After filtration under reduced pressure and crystallization from methanol to eliminate other impurities, 2-((1-chloro-9-oxo-9*H*-thioxanthen-4-yl)oxy)acetic acid (**5**) was obtained in 48 % yield (23.2 mg).

3.2.4. Synthesis of 1-[2-(diethylamino)ethyl]-amino-4-propoxy-9*H*-thioxanthen-9-one (**6**)

The synthesis of aminothioxanthone 6 was performed via a copper-catalysed nucleophilic aromatic substitution (Ullmann-type C-N coupling) of chlorine on carbon 1 of compound **5** with *N,N*-diethylethane-1,2-diamine (Scheme 6)[12].This CuI-catalysed reaction took place in a methanolic and alkaline environment (K_2CO_3), without stirring, at 100 °C in a closed vessel reactor. The carbonate group of the K_2CO_3 chelate the surplus CuI, a catalytic agent usually used in this type of reactions[18].

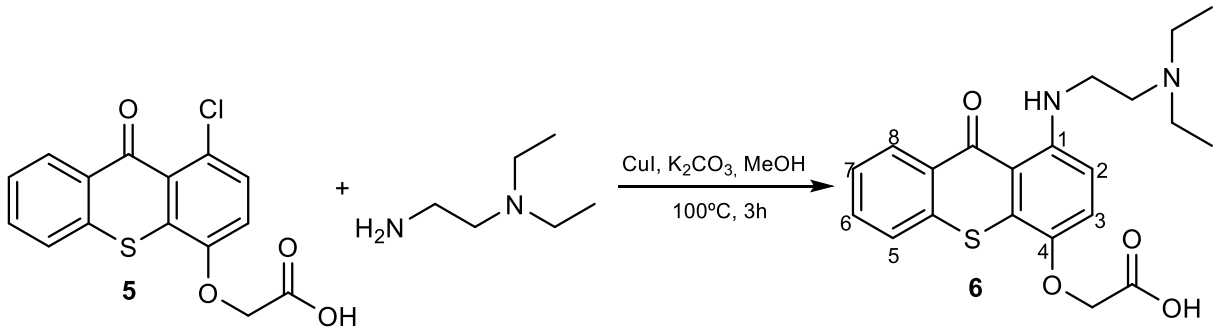

Scheme 6 - Synthesis of 1-[2-(diethylamino)ethyl]-amino-4-propoxy-9*H*-thioxanthen-9-one (**6**).

The reaction was monitored by TLC analysis using a mixture of CH_2Cl_2:MeOH (7:3) as mobile phase and was observed under UV light at 254 and 365 nm. After 3 hours the reaction was completed and after cooling to room temperature, the methanol was evaporated under reduced pressure. The product was redissolved in ethyl acetate and extracted from water to remove the CuI and K_2CO_3.The organic layer was dried with anhydrous sodium sulphate, filtered and evaporated. The purification and isolation of compound **6** wasn't carried out due to time limitations.

3.3. Structure elucidation

The structure elucidation of the synthesized compounds (**1**-**5**) was established by infrared (IR) spectroscopy and nuclear magnetic resonance (NMR). Whenever needed, the ^{13}C NMR assignments were confirmed by bidimensional heteronuclear single quantum correlation (2D HSQC) and heteronuclear multiple bond correlation (HMBC).

3.3.1. IR spectroscopy

Tables 2 and 3 present the maximum wavenumber of the IR spectroscopy bands for the synthesized compounds.

Table 2 - IR data for compound **1** and **2**.

Compound	Group	Wavenumber (cm^{-1})
Compound 1	N-H	3344.17
	O-H	3204.83
	C-H (Ar)	3033.71
	C-H	2927.04, 2883.42, 2850.55
	C=O	1756.21
	C=C (Ar)	1573.90, 1528.66
Compound 2	N-H	3381.49
	C-H (Ar)	3033.04
	C-H	2926.19, 2850.17
	C=O	1651.64
	C=C (Ar)	1574.71, 1538.32

The IR data of compounds **1** and **2** indicate the presence of the band corresponding to the N-H (3344.17 cm^{-1} and 3381.49 cm^{-1}, respectively). It was also detected the characteristic bands of the aromatic bond C=C (3381.49 - 1574.71 cm^{-1}) and C-H bond (3033.04, 3033.71 cm^{-1}). The bands corresponding C-H bonds (2850.17 - 2927.04 cm^{-1}) of the aliphatic chains were detected. Both compounds also present a band corresponding to a C=O bond (1756.21 cm-1 and 1651.64 cm^{-1}), which are observed in the spectra. Compound **1** also present the characteristic band corresponding to the O-H bond (3204.83 cm^{-1}).

Table 3 - IR data for compound **3** and **4**

Compound	Group	Wavenumber (cm^{-1})
Compound 3	O-H	3261.36
	C-H (Ar)	3036.32
	C=O	1630.95
	C=C (Ar)	1584.75, 1570.17, 1557.49
Compound 4	C-S	3439.90
	C-H	2955.53, 2923.68, 2850.83
	C=O	1639.5
	C=C (Ar)	1763.98

The IR data of compounds **3** and **4** presented the bands corresponding to the C=O (1630.95 cm^{-1} and 1639.5 cm^{-1}, respectively) and the aromatic bonds C=C (1584.75 - 1557.49 cm^{-1} and 1763.98 cm^{-1}, respectively). Compound **3** also presented the band characteristic of the aromatic C-H bonds (3036.32

cm^{-1}) and the O-H bond (3261.36 cm^{-1}). To confirm the formation of compound **4**, no band corresponding to O-H could be observed. In IR data of compound **4** was detected the band corresponding to the C-S bond (3439.90 cm^{-1}), which didn´t show up in the IR data of compound **3**, probably because it was hidden by the band corresponding to the O-H bond.
The IR data of compound **5** wasn't carried out due to time limitations.

3.3.2. ^{1}H NMR – Proton nuclear magnetic resonance

Figures 15-19 (in section 7. Supporting Information) and Tables 4 and 5 present the chemical shifts of the ^{1}H NMR signals for the synthesized compounds.

Table 4 - Chemical shifts (δ_H, ppm), multiplicity and coupling constants (*J*, Hz) of the ^{1}H NMR spectra of compound **1** and **2**.

Position	δ_H (ppm)		Position
	Compound 1	Compound 2	
H-c	1.67, p, *J* = 7.0 Hz		
H-d	2.27, t, *J* = 7.2 Hz	2.15, t, *J* = 6.1 Hz	H-c
H-b	3.30, q, *J* = 6.7 Hz	3.26, q, *J* = 6.1 Hz	H-b
Ar-$\underline{CH_2}$	5.16; 5.10, s	5.05; 5.12, s	Ar-$\underline{CH_2}$
H-4	7.15, s	7.14 – 7.08, m	H-4, H-5
H-5	7.16, d, *J* = 2.2 Hz		
$\underline{Ar}$-CH_2	7.51 – 7.32, m, *J* = 6.7 Hz	7.44 – 7.26, m	$\underline{Ar}$-CH_2
H-6	7.73, dd, *J* = 5.8, 3.8 Hz	7.67, m	H-6
-OH	8.11, s	8.03, t *J* = 5.2 Hz	-NH

In the ^{1}H NMR spectra of both compounds **1** and **2**, at δ=7.26 ppm appears the characteristic signal corresponding to the solvent used, $CDCl_3$. Since compounds **1** and **2** were obtained from the 2,3-bis(benzyloxy)benzoic acid, they presented the signals corresponding to the aromatic protons of the catechol group – H-4, H-5 (δ = 7.08 – 7.16 ppm) and H-6 (δ = 7.73 – 7.67 ppm) – and the protons of the benzyl protected groups – $\underline{Ar}$-CH_2 (δ = 7.26 – 7.56 ppm) and Ar-$\underline{CH_2}$ (δ = 5.05 – 5.16 ppm). However, it's to highlight that these signals in compound **2** have a higher integration (2-fold) than those of compound **1** due to the symmetry of compound **2**.
In the ^{1}H NMR spectrum of compound **1** (Figure 9), a broad singlet with the highest value of chemical shift (δ_H = 8.11 ppm) was observed, confirming the presence of the proton of the hydroxyl group of the carboxylic acid. Another proton that would be expected in this zone, would be the amide proton, however, sometimes it's not detected, due to the interchangeable nature. The signal that was observed with the chemical shift of 3.30 ppm confirmed the presence of H-b, which has a higher chemical shift than H-d e H-c, because it's closer to the nitrogen and oxygen atoms of the amide group, that cause an electronegative effect. The signals that were observed with the chemical shift of 2.27 ppm and 1.67 ppm confirmed the presence to H-d and H-c, respectively. The H-d originates a higher chemical shift because, it's close to two oxygen atoms.
For compound **2**, the proton of -NH was confirmed by the presence of a signal with the highest chemical shift (δ_H = 8.03 ppm), due to the effect of the carbonyl group, resulting in deprotection of the proton. The H-b possessed a similar chemical shift to compound **1** (δ_H = 3.26 ppm), since it's also directly linked to the amide. However, the H-c shows a slightly lower chemical shift (δ_H = 2.15 ppm) than the H-d of the compound 1, because only was deprotected by the nitrogen atom.

Table 5 - Chemical shifts (δ_H, ppm), multiplicity and coupling constants (*J*, Hz) of the ^{1}H NMR spectra of compound **3**, **4** and **5**.

Position	δ_H (ppm)		
	Compound 3	**Compound 4**	**Compound 5**
H-4'''		3.73, s	
H-4'		5.13, s	5.00, s
H-2	7.43, d, *J* = 8.6 Hz	7.55, d, *J* = 8.7 Hz	7.54, d, *J* = 8.6 Hz
H-3	7.14, d, *J* = 8.6 Hz	7.36, d, *J* = 8.6 Hz	7.32, d, *J* = 8.8 Hz
H-5	7.81, ddd, *J* = 8.1, 1.3, 0.6 Hz	7.84, ddd, *J* = 8.1, 1.2, 0.6 Hz	7.84, dd, *J* = 8.2, 1.2 Hz
H-6	7.73, ddd, *J* = 8.2, 7.0, 1.5 Hz	7.73 – 7.78, m	7.76, ddd, *J* = 8.2, 7.1, 1.5 Hz
H-7	7.55, ddd, *J* = 8.2, 7.0, 1.3 Hz	7.58, dd, *J* = 7.6, 1.7 Hz	7.60 – 7.56, m
H-8	8.27, ddd, *J* = 8.0, 1.5, 0.5 Hz	8.28, ddd, *J* = 8.0, 1.5, 0.5 Hz	8.27, dd, *J* = 8.1, 1.4 Hz
-OH	11.41, s		

In the ^{1}H NMR spectra of compounds **3**, **4** and **5**, at 2.50 ppm it was verified the characteristic signal of the solvent DMSO-d_6. All these three thioxanthone derivatives present the characteristic signals of the thioxanthone scaffold, therefore, the chemical shift and coupling constants of the aromatic protons – H-2, H-3, H-5, H-6, H-7 and H-8 (δ = 7.14–8.28 ppm) – were very similar.
For compound **3**, a broad singlet with the highest chemical shift of 11.41 ppm, confirms the presence of the proton to the -OH group at the C-4 position. Since compound **4** resulted from compound 3, the presence of the signals corresponding to H-4' and H-4''' confirms its formation. The signal that corresponds to the resonance of H-4' was observed at a higher chemical shift (δ = 5.13 ppm) than H-4''' (δ = 3.73 ppm), since it was surrounded by a more electronegative environment provided by oxygen atoms, which resulted in the highest deprotection. Once more, as compound **5** resulted from the demethylation of compound **4**, signals that would correspond to the protons of the -CH_3 group could not be observed. Sometimes, the signal of -OH wasn't shown, as in the spectrum of the compound **5** since it shared the proton to the oxygen of the water, which exists in the solvent.

3.3.3. ^{13}C NMR – Carbon Nuclear Magnetic Resonance

Figures 20-23 (in section 7. Supporting Information) and Tables 6 and 7 present the chemical shifts of the ^{13}C NMR signals for the synthesized compounds **1-5**.

Table 6 - Chemical shifts (δ_C, ppm) of the ^{13}C NMR spectra of compound **1** and **2**.

Position	δ_C (ppm)	
	Compound 1	**Compound 2**
Ar-CH_2	127.7	127.8 – 128.8
C_{Ar}-CH_2	136.2, 136.3	136.0
Ar-CH_2	71.3, 76.6	71.4, 76.4
C-1	126.7	127.7
C-2	146.9	147.0
C-3	151.7	151.9
C-4	117.2	117.1
C-5	128.9	124.5
C-6	128.3	123.3

C-d	31.6	
C-c	25.0	48.2
C-b	38.7	39.5
C-a	165.9	166.3

In the ^{13}C NMR spectra of both of compounds **1** and **2**, at $\delta = 77$ ppm was observed the signal corresponding to the solvent $CDCl_3$. As verified from the ^{1}H NMR spectra these compounds had characteristic signals corresponding to the carbons of the catechol group – C-1, C-2, C-3, C-4, C-5 and C-6 (δ = 117.1 – 127.7 ppm, 128.3 ppm, 128.9 ppm and 146.9 – 151.9 ppm, respectively) – and the carbons of the benzyl protected groups – $\underline{Ar}$-CH_2 (δ = 127.7 – 128.8 ppm), $\underline{C}_{Ar}$-CH_2 (δ = 136.0 – 136.3 ppm) and Ar-$\underline{CH_2}$ (δ = 71.3 – 76.6 ppm).

In both spectra, the signal that appears at the highest chemical shift (δ = 165.9 ppm and 166.3 ppm, for compound **1** and **2**, respectively), confirmed the presence of the carbonyl carbon at position C-a, due to the inductive effect of the oxygen atom, resulting in a higher deprotection. In the ^{13}C NMR spectrum of compound **1,** of the signals at δ = 38.7 ppm, 31.6 ppm and 25.0 ppm correspond to the resonance of C-b, C-d and C-c, respectively. Among these, the carbon in the position C-b was the most deprotected due to the nitrogen and carbonyl group pf the amide, resulting in a signal with the highest chemical shift. The signal of C-d has a higher chemical shift than the C-c, since it's closer to the oxygens of the carboxylic acid.

In the ^{13}C NMR spectrum of compound **2**, the carbons in the positions C-b and C-c were confirmed by the presence of the signals at δ = 39.5 ppm and δ = 48.2 ppm.

Table 7 - Chemical shifts (δ, ppm) of the ^{13}C NMR spectra of compounds **4** and **5**.

Position	**δ_C (ppm)**	
	Compound 4	**Compound 5**
C-1	135.1	135.1
C-2	115.2	114.9
C-3	129.3	129.2
C-4	151.8	151.9
C-5	126.2	126.1
C-6	133.2	133.2
C-7	127.0	126.9
C-8	129.7	129.6
C-9	179.6	179.6
C-4a	130.0	130.0
C-5a	127.0	126.6
C-8a	130.5	130.5
C-9a	127.6	127.6
C-4’	66.4	66.2
C-4’’	168.9	169.8
C-4’’’	52.6	

Compound **3** was already synthesized by Cardoso *et al.*, therefore, it was enough to compare the ^{1}H NMR spectra to confirm the identity of this compound.

In ^{13}C NMR spectra of compounds **4** and **5**, at δ = 40 ppm it was verified the characteristic signal of the solvent DMSO-d_6. Since these compounds are thioxanthones derivatives, they present the characteristic signals of the thioxanthone scaffold – C-1, C-2, C-3, C-4, C-5, C-6, C-7, C-8, C-9, C-4a, C-5a, C-8a and C-9a (δ = 114.9 – 135.1 ppm). The signals at highest chemical shifts of δ = 168.9 ppm and δ = 169.8 ppm were observed on both spectra which confirmed the presence of the carbon on the position of C-4’’, since they belong to carbonyl group. To confirm the formation of compound **4**, in the

respective spectrum the presence of a signal with the chemical shift of 52.3 ppm was verified corresponding to the position of C-4'''.
To confirm the formation of compound 5, no chemical shift around δ = 52 ppm could be observed.

4. Materials and Methods

4.1. Chemistry

All reagents and solvents were purchased from Sigma-Aldrich (St. Louis, MO, USA), Alfa Aesar (Ward Hill, MA, USA), Pronalab (State of Mexico, México), TCI (Tokyo, Japan), Acros Organics (Thermo Fisher Scientific, Geel, Belgium), Fisher Scientific (Thermo Fisher Scientific, Loughborough, UK), Chem-Lab NV (Zedelgem, Belgium), or Honeywell Riedel-de Haën (Seelze, Germany), and no further purification process was implemented. Solvents were evaporated using a rotary evaporator under reduced pressure (Buchi Waterchath B-480, BÜCHI Labortechnik AG, Flawil, Switzerland). Reaction progressions were controlled by thin layer chromatography (TLC) using Merck silica gel 60 (GF_{254}) precoated plates (0.2 mm of thickness) with appropriate mobile phases. Compounds were visually detected at 254 and 365 nm, and chemicals were used for the visualization of chromatograms (ninhydrin and iron(III) chloride soluction). Purifications of the synthesized compounds were performed by flash column chromatography using silica gel 60 (0.040–0.063 mm, Merck, Darmstadt, Germany). Infrared (IR) spectra were measured in KBr microplates in a Fourier transform infrared spectroscopy spectrometer Nicolet iS10 from Thermo Scientific with Smart OMNI-Transmisson accessory (Software OMNIC 8.3). The ^{1}H and ^{13}C NMR spectra were performed at the University of Aveiro, Department of Chemistry on a Bruker Avance 300 spectrometer (300.13 and for ^{1}H and 75.47 MHz for ^{13}C, Bruker Biosciences Corporation, Billerica, MA, USA) or at the Centro de Materiais da Antibiotics 2022, 11, 1488 14 of 22 Universidade do Porto (CEMUP) on a Bruker Avance III 400 spectrometer (400 MHz) in $CDCl_3$ or DMSO-d_6 (Deutero GmbH, Ely, UK) at room temperature. Chemical shifts are expressed in δ (ppm) values relative to tetramethylsilane (TMS) as an internal reference. Coupling constants are reported in hertz (Hz). ^{13}C NMR assignments were made by 1D, 2D Heteronuclear Single Quantum Coherence (HSQC) and Heteronuclear Multiple Bond Correlation (HMBC) NMR experiments (long-range C, H coupling constants were optimized to 7 Hz). The following compounds were synthesized and purified by the described procedures.

4.2. Synthesis of siderophore mimetics

4.2.1. Synthesis of 4-(2,3-bis(benzyloxy)benzamide)butanoic acid (**1**)

The synthesis of compound **1** was performed according to Joaqui-Joaqui *et al.* [9] with some modifications. A solution of DCC) (308.5 mg, 1.50 mmol) in dry THF (2 mL) was added dropwise to a mixture of 2,3-bis(benzyloxy)benzoic acid (500 mg, 1.50 mmol) and NHS (206.5 mg, 1.79 mmol) in dry THF (5 mL) at 0 °C. The mixture was stirred for 3 hours at room temperature and was filtered. The filtrate was added to a solution of 4-amino-butanoic acid (154.2 mg. 1.50 mmol) and $KHCO_3$ (299.4 mg, 2.99 mmol) in 50 % aqueous THF (50 mL) at pH ~8. After stirring the reaction mixture at room temperature for 24 hours, the THF was removed. The residue was treated with 0.5 M citric acid (50 mL) and extracted with ethyl acetate (2 x 50 mL). The organic layer was washed with water (50 mL) and brine (50 mL). Purification by flash chromatography (SiO_2, CH_2Cl_2:MeOH 9:1) gave the pure product.

4-(2,3-bis(Benzyloxy)benzamide)butanoic acid (**1**): white solid (489.4 mg, 78 %). m.p. 181.7-183.3 °C; IR (KBr) υ_{max}: 3344.17, 3204.83, 3033.71, 2927.04. 2882.42, 2850.55, 1756.21, 1573.90, 1528.66; ^{1}H NMR (300.13 MHz, $CDCl_3$): δ = 8.11 (1H, s, -OH), 7.73 (1H, dd, *J* = 5.8 and 3.8 Hz, H-6), 7.51–7.32 (10H, m, Ar-CH_2), 7.16 (1H, d, *J* = 2.2 Hz, H-5), 7.15 (1H, s, H-4), 5.16 (2H, s, Ar-CH_2), 5.10 (2H, s, Ar-CH_2), 3.30 (2H, q, *J* = 6.7 Hz, H-b), 2.27 (2H, t, *J* = 7.2 Hz, H-d), 1.67 (2H, p, *J* = 7.0 Hz, H-c); ^{13}C NMR (75.47 MHz, $CDCl_3$): δ = 165.9 (C-a), 151.7 (C-3), 146.9 (C-2), 136.3 (C_{Ar}-CH_2), 136.2 (C_{Ar}-CH_2), 128.9 (C-5), 128.3 (C-6), 127.7 (Ar-CH_2), 126.7 (C-1), 117.2 (C-4), 76.6 (Ar-CH_2), 71.3 (Ar-CH_2), 38.7 (C-b), 31.6 (C-d), 25.0 (C-c).

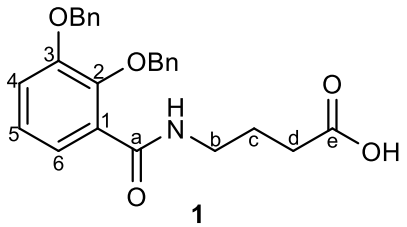

Figure 10 - Structure of 4-(2,3-bis(benzyloxy)benzamide)butanoic acid (**1**), with the respective numbering.

4.2.2. Synthesis of *N,N'*-(azanediylbis(ethane-2,1-diyl))bis(2,3-bis(benzyloxy)benzamide (**2**)

The synthesis of compound **2** was performed according to Yoganathan *et al*.[10] and Sharma *et al.*[11] with some modifications. To a solution of 2,3-bis(benzyloxy)benzoic acid (1.5 mg, 4.49 mmol) in dry CH_2Cl_2 (30 mL), CDI (1.45 g, 8.97 mmol) was added and the reaction mixture was stirred for 2 hours at room temperature. A solution of diethylenetriamine (0.38 mL, 3.59 mmol) in dry CH_2Cl_2 (1 mL) was then added to the flask. The reaction mixture was then concentrated and the crude product was purified by flash column chromatography (SiO_2, CH_2Cl_2:MeOH 9:1) to obtain the pure product.

N,N'-(Azanediylbis(ethane-2,1-diyl))bis(2,3-bis(benzyloxy)benzamide (**2**): pale yellow oil (2.5216 g, 72 %). m.p. 129.5-131.3 °C; IR (KBr) υ_{max}: 3381.49, 3033.04, 2926.19, 2850.17, 1651.64, 1574.71, 1538.32; ^{1}H NMR (400 MHz, $CDCl_3$): δ = 8.03 (2H, t, *J* = 5.2 Hz, -NH), 7.67 (2H, m, H-6), 7.44-7.26 (16H, m, Ar-CH_2), 7.11-7.08 (4H, m, H-4), 5.16 (2H, s, H-4, H-5), 5.12 (4H, s, Ar-CH_2), 5.05 (4H, s, Ar-CH_2), 3.26 (4H, q, *J* = 6.1 Hz, H-b), 2.51 (4H, t, *J* = 6.1 Hz, H-c); ^{13}C NMR (75.47 MHz, $CDCl_3$): δ = 166.3 (C-a), 151.9 (C-3), 147.0 (C-2), 136.0 (C_{Ar}-CH_2), 127.8, 128.7, 128.80, 128.8, 128.4 (Ar-CH_2), 127.7 (C-1), 124.5 (C-5), 123.3 (C-6), 117.1 (C-4), 76.4 (Ar-CH_2), 71.4 (Ar-CH_2), 48.2 (C-c), 39.5 (C-b).

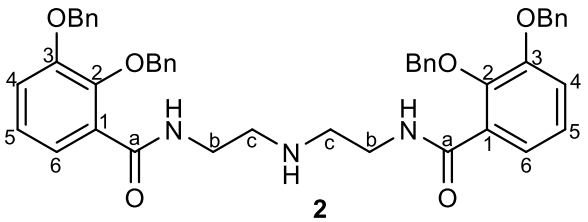

Figure 11 - Structure of *N,N'*-(azanediylbis(ethane-2,1-diyl))bis(2,3-bis(benzyloxy)benzamide (**2**), with the respective numbering.

4.3. Synthesis of thioxanthone derivatives

4.3.1. Synthesis of the 1-chloro-4-hydroxy-9*H*-thioxanthen-9-one (**3**)

The synthesis of compound **3** was performed according to Cardoso *et al*. [12] with some modifications. To a solution of commercial 1-chloro-4-propoxy-9*H*-thioxanthen-9-one (1.5 mg, 4.92 mmol) in dry CH_2Cl_2 (20 mL) was carefully and gradually added $AlCl_3$ (1.97 g, 14.76 mmol) under a nitrogen atmosphere. The reaction mixture was heated at 40 °C for 24 hours. At the end of the reaction, the mixture was extracted with 20 % NaOH and 5 % HCl to give the pure product.

1-Chloro-4-hydroxy-9*H*-thioxanthen-9-one (**3**): greenish-yellow solid (1.1 g, 87 %). m.p. 236.9–239.3 °C; IR (KBr) υ_{max}: 3261.36, 3063.32, 1630.95, 1584.75, 1570.17, 1557.49, 1225.40, 1081.37; ^{1}H NMR (400 MHz, DMSO-d6): δ = 11.41 (1H, s, -OH), 8.27 (1H, ddd, J = 8.0, 1.5, 0.5 Hz, H-8), 7.81 (1H, ddd, J = 8.1, 1.3, 0.6 Hz, H-5), 7.73 (1H, ddd, J = 8.2, 7.0, 1.5 Hz, H-6), 7.55 (1H, ddd, J = 8.2, 7.0, 1.3 Hz, H-7), 7.43 (1H, d, J = 8.6 Hz, H-2), 7.14 (1H, d, J = 8.6 Hz, H-3).

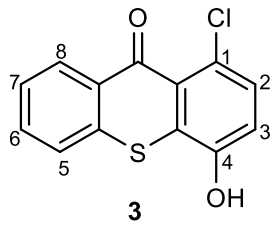

3

Figure 12 - Structure of 1-chloro-4-hydroxy-9*H*-thioxanthen-9-one (**3**), with the respective numbering.

4.3.2. Synthesis of methyl 2-((1-chloro-9-oxo-9*H*-thioxanthen-4-yl)oxy)acetate (**4**)

The synthesis of compound **4** was performed according to Durães *et al.* [13]. Methyl bromoacetate ($BrCH_2COOCH_3$, 21 µL, 0.23 mmol) was added to a solution of 1-chloro-4-hydroxy-9*H*-thioxanten-9-one (**3**, 50 mg, 0.19 mmol) and K_2CO_3 (26.1 mg, 0.19 mmol) in dry acetone (8 mL). The mixture was refluxed and stirred for 24 hours. The mixture was then concentrated under reduced pressure and extracted with ethyl acetate (2 × 100 mL) and water (2 × 100 mL) to give the desirable product as an orange-brown solid.

Methyl 2-((1-chloro-9-oxo-9*H*-thioxanthen-4-yl)oxy)acetate (**4**): orange-brown solid (61.9 mg, 97 %). m.p. 171.3–173.6 °C; IR (KBr) υ_{max}: 3439.90, 3008.11, 2955.53, 2923.68, 2850.83, 1763.98, 1639.52; ^{1}H NMR (400 MHz, DMSO-d_6): δ = 8.28 (1H, ddd, *J* = 8.0, 1.5, 0.6 Hz, H-8), 7.84 (1H, ddd, *J* = 8.1, 1.2, 0.6 Hz, H-5), 7.78–7.73 (1H, m, H-6), 7.58 (1H, dd, *J* = 7.6, 1.7 Hz, H-7), 7.55 (1H, d, *J* = 8.7 Hz, H-2), 7.36 (1H, d, *J* = 8.8 Hz, H-3), 5.13 (2H, s, H-4'), 3.73 (3H, s, H-4'''); ^{13}C NMR (75.45 MHz, DMSO-d_6): δ = 179.6 (C-9), 168.9 (C-4''), 151.8 (C-4), 135.1 (C-1), 133.2 (C-6), 130.5 (C-8a), 130.0 (C-4a), 129.7 (C-8), 129.3 (C-3), 127.6 (C-9a), 127.0 (C-7, C-5a), 126.2 (C-5), 115.2 (C-2), 66.4 (C-4'), 52.6 (C-4''').

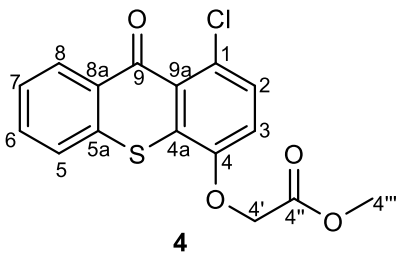

4

Figure 13 - Structure of methyl 2-((1-chloro-9-oxo-9*H*-thioxanthen-4-yl)oxy)acetate (**4**), with the respective numbering

4.3.3. Synthesis of 2-((1-chloro-9-oxo-9*H*-thioxanthen-4-yl)oxy)acetic acid (**5**)

The synthesis of compound **5** was performed according to Durães *et al.* [13]. To a solution of methyl 2-((1-chloro-9-oxo-9*H*-thioxanthen-4-yl)oxy)acetate (**4**, 50 mg, 0.15 mmol) in CH_2Cl_2/MeOH (1:1 v/v, 10 mL), 5 M NaOH (3 mL) was added. The mixture was kept at room temperature and stirred for 24 hours. Subsequently, the organic solvents were evaporated under reduced pressure and water (30 mL) was added. The aqueous phase was acidified with 5 M HCl solution, resulting in the formation of a precipitate which was collected by filtration under reduced pressure. It was then washed with water and crystallized from MeOH to give the pure product.

2-((1-Chloro-9-oxo-9*H*-thioxanthen-4-yl)oxy)acetic acid (**5**): yellowish orange solid (61.9 mg, 97 %); ^{1}H NMR (400 MHz, DMSO-d_6): δ = 8.27 (1H, dd, *J* = 8.1, 1.4 Hz, H-8), 7.84 (1H, dd, *J* = 8.2, 1.2 Hz, H-5), 7.74 (1H, ddd, *J* = 8.2, 7.1, 1.5 Hz, H-6), 7.60–7.56 (1H, m, H-7), 7.54 (1H, d, *J* = 3.6 Hz, H-2), 7.32 (1H, d, *J* = 8.8 Hz, H-3), 5.00 (2H, s, H-4'); ^{13}C NMR (75.45 MHz, DMSO-d_6): δ = 179.6 (C-9), 169.8 (C-4''), 151.9 (C-4), 135.1 (C-1), 133.2 (C-6), 130.5 (C-8a), 130.0 (C-4a), 129.6 (C-8), 129.2 (C-3), 127.6 (C-9a), 126.9 (C-7), 126.6 (C-5a), 126.1 (C-5), 114.9 (C-2), 66.2 (C-4').

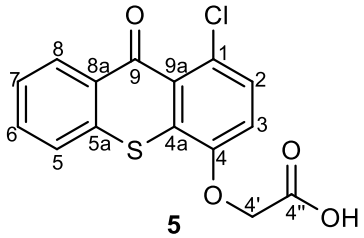

5

Figure 14 - Structure of 2-((1-chloro-9-oxo-9*H*-thioxanthen-4-yl)oxy)acetic acid (**5**), with the respective numbering.

4.3.4. Synthesis of 1-[2-(diethylamino)ethyl]-amino-4-propoxy-9*H*-thioxanthen-9-one (**6**)

The synthesis of compound **6** was performed according to Cardoso *et al.* [12]. To a mixture of 2-((1-chloro-9-oxo-9*H*-thioxanthen-4-yl)oxy)acetic acid (**5**, 10 mg, 0.03 mmol) and *N*,*N*-diethylethane-1,2-diamine (9 µL, 0.06 mmol) dissolved in MeOH was added CuI (5.90 mg, 0.03 mmol) and K_2CO_3 (4.28 mg, 0.03 mmol). The reaction mixture was heated at 100 °C in a closed vessel reactor for 3 hours. After completing the reaction, MeOH was evaporated and the residue was dissolved in ethyl acetate and extracted from water.

5. Conclusion and Future Perspectives:

The objectives of this project were to synthesize two mimetic siderophores and a thioxanthone derivatives, which were achieved, despite some difficulties in the purification of the aminothioxanthone **6**.

The synthesis of siderophores **1** and **2** and their elucidation were well achieved, obtaining good yields. As a perspective for the future, it would be interesting to use compound **1** as a starting material to synthesize another mimetic siderophore with a potential additional site to bind the linker, usually an amine group.
The synthesis and the structure elucidation of the thioxanthones derivatives **3**-**5**, were also well achieved, however it wasn't possible to purify the aminothioxanthone **6**. In the future it's necessary to repeat these syntheses with new purification strategies. In addition, it is also necessary to perform studies on the activity of the thioxanthone **5** and **6** to confirm their antimicrobial activity.
Another important following step as future perspective is the conjugation of the *N,N*'-(azanediylbis(ethane-2,1-diyl))bis(2,3-bis(benzyloxy)benzamide) (**2**) with the synthesized aminothioxanthone (**6**) in order to obtain the siderophore-antimicrobial conjugate with a potential activity against resistance to antimicrobials.

6. References:

(1) Almeida, M. C.; da Costa, P. M.; Sousa, E.; Resende, D. Emerging Target-Directed Approaches for the Treatment and Diagnosis of Microbial Infections. *J Med Chem* **2023**, *66* (1), 32-70. DOI: 10.1021/acs.jmedchem.2c01212 .

(2) Duraes, F.; Palmeira, A.; Cruz, B.; Freitas-Silva, J.; Szemeredi, N.; Gales, L.; da Costa, P. M.; Remiao, F.; Silva, R.; Pinto, M.; et al. Antimicrobial Activity of a Library of Thioxanthones and Their Potential as Efflux Pump Inhibitors. *Pharmaceuticals (Basel)* **2021**, *14* (6). DOI: 10.3390/ph14060572 .

(3) Kurth, C.; Kage, H.; Nett, M. Siderophores as molecular tools in medical and environmental applications. *Org Biomol Chem* **2016**, *14* (35), 8212-8227. DOI: 10.1039/c6ob01400c .

(4) Ahmed, E.; Holmstrom, S. J. Siderophores in environmental research: roles and applications. *Microb Biotechnol* **2014**, *7* (3), 196-208. DOI: 10.1111/1751-7915.12117 .

(5) Hider, R. C.; Kong, X. Chemistry and biology of siderophores. *Nat Prod Rep* **2010**, *27* (5), 637-657. DOI: 10.1039/b906679a .

(6) Syed, Y. Y. Cefiderocol: A Review in Serious Gram-Negative Bacterial Infections. *Drugs* **2021**, *81* (13), 1559-1571. DOI: 10.1007/s40265-021-01580-4.

(7) Sato, T.; Yamawaki, K. Cefiderocol: Discovery, Chemistry, and In Vivo Profiles of a Novel Siderophore Cephalosporin. *Clin Infect Dis* **2019**, *69* (Suppl 7), S538-s543. DOI: 10.1093/cid/ciz826.

(8) Negash, K. H.; Norris, J. K. S.; Hodgkinson, J. T. Siderophore-Antibiotic Conjugate Design: New Drugs for Bad Bugs? *Molecules* **2019**, *24* (18). DOI: 10.3390/molecules24183314.

(9) Bessa, L. J.; Palmeira, A.; Gomes, A. S.; Vasconcelos, V.; Sousa, E.; Pinto, M.; Martins da Costa, P. Synergistic Effects Between Thioxanthones and Oxacillin Against Methicillin-Resistant Staphylococcus aureus. *Microb Drug Resist* **2015**, *21* (4), 404-415. DOI: 10.1089/mdr.2014.0162.

(10) Pinto, M. M. M.; Palmeira, A.; Fernandes, C.; Resende, D. I. S. P.; Sousa, E.; Cidade, H.; Tiritan, M. E.; Correia-da-Silva, M.; Cravo, S. From Natural Products to New Synthetic Small Molecules: A Journey through the World of Xanthones. *Molecules* **2021**, *26* (2), 431.

(11) Palmeira, A.; Vasconcelos, M. H.; Paiva, A.; Fernandes, M. X.; Pinto, M.; Sousa, E. Dual inhibitors of P-glycoprotein and tumor cell growth: (re)discovering thioxanthones. *Biochem Pharmacol* **2012**, *83* (1), 57-68. DOI: 10.1016/j.bcp.2011.10.004.

(12) Joaqui-Joaqui, M. A.; Pandey, M. K.; Bansal, A.; Raju, M. V. R.; Armstrong-Pavlik, F.; Dundar, A.; Wong, H. L.; DeGrado, T. R.; Pierre, V. C. Catechol-Based Functionalizable Ligands for Gallium-68 Positron Emission Tomography Imaging. *Inorg Chem* **2020**, *59* (17), 12025-12038. DOI: 10.1021/acs.inorgchem.0c00975.

(13) Yoganathan, S.; Sit, C. S.; Vederas, J. C. Chemical synthesis and biological evaluation of gallidermin-siderophore conjugates. *Org Biomol Chem* **2011**, *9* (7), 2133-2141. DOI: 10.1039/c0ob00846j.

(14) Sharma, S. K.; Miller, M. J.; Payne, S. M. Spermexatin and spermexatol: new synthetic spermidine-based siderophore analogs. *Journal of Medicinal Chemistry* **1989**, *32* (2), 357-367. DOI: 10.1021/jm00122a013.

(15) Cardoso, J.; Freitas-Silva, J.; Duraes, F.; Carvalho, D. T.; Gales, L.; Pinto, M.; Sousa, E.; Pinto, E. Antifungal Activity of a Library of Aminothioxanthones. *Antibiotics (Basel)* **2022**, *11* (11). DOI: 10.3390/antibiotics11111488.

(16) Duraes, F.; Cravo, S.; Freitas-Silva, J.; Szemeredi, N.; Martins-da-Costa, P.; Pinto, E.; Tiritan, M. E.; Spengler, G.; Fernandes, C.; Sousa, E.; et al. Enantioselectivity of Chiral Derivatives of Xanthones in Virulence Effects of Resistant Bacteria. *Pharmaceuticals (Basel)* **2021**, *14* (11). DOI: 10.3390/ph14111141.

(17) Hermanson, G. T. Chapter 4 - Zero-Length Crosslinkers. In *Bioconjugate Techniques (Third Edition)*, Hermanson, G. T. Ed.; Academic Press, 2013; pp 259-273.

(18) Yang, Y. Side Reactions Upon Amino Acid/Peptide Carboxyl Activation. 2016; pp 95-118.

(19) Arifin, B.; Tang, D.; Achmadi, S. Transformation of Eugenol and Safrole into Hydroxychavicol. *Indonesian Journal of Chemistry* **2015**, *15*, 77-85. DOI: 10.22146/ijc.21227.

(20) Phyo, Y. Z.; Teixeira, J.; Tiritan, M. E.; Cravo, S.; Palmeira, A.; Gales, L.; Silva, A. M. S.; Pinto, M. M. M.; Kijjoa, A.; Fernandes, C. New chiral stationary phases for liquid chromatography based on small molecules: Development, enantioresolution evaluation and chiral recognition mechanisms. *Chirality* **2020**, *32* (1), 81-97. DOI: 10.1002/chir.23142.

(21) Weidlich, T.; Špryncová, M.; Čegan, A. Copper-Catalyzed Reactions of Aryl Halides with N-Nucleophiles and Their Possible Application for Degradation of Halogenated Aromatic Contaminants. In *Catalysts*, **2022**; *12*.

7. Supporting Information

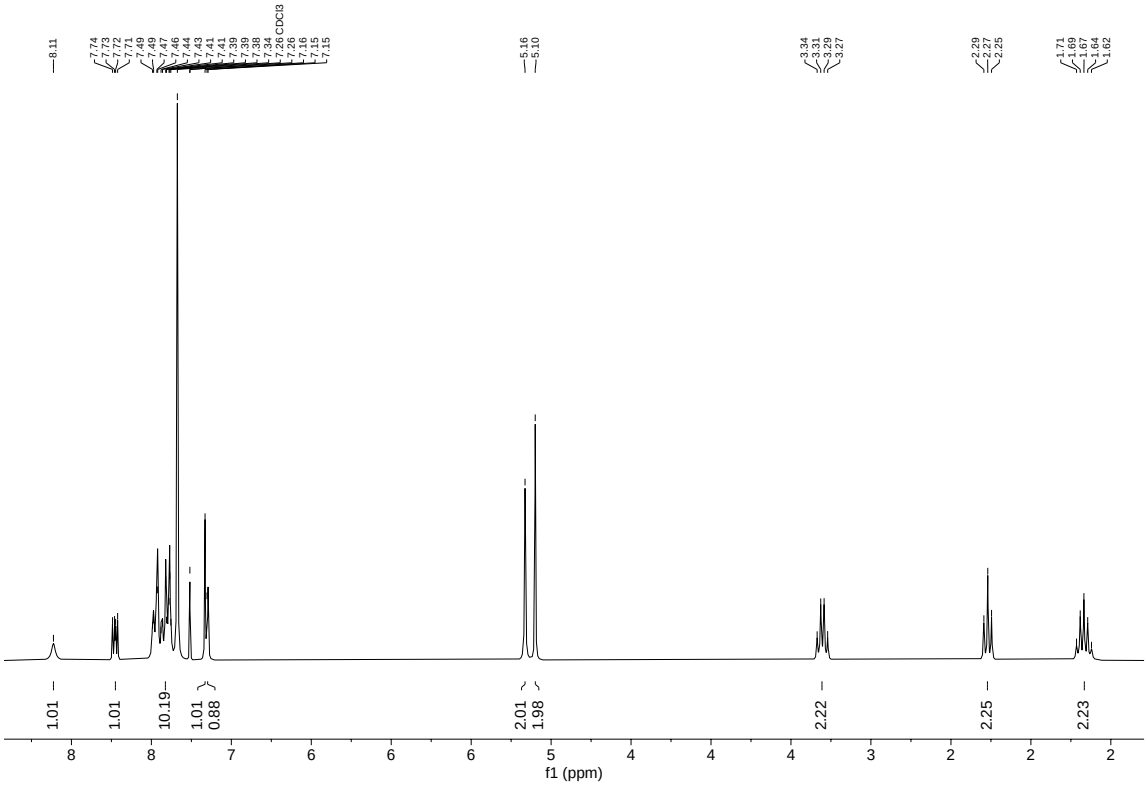

Figure 15 - ^{1}H NMR spectrum of compound **1** ($CDCl_3$, 300.13 MHz).

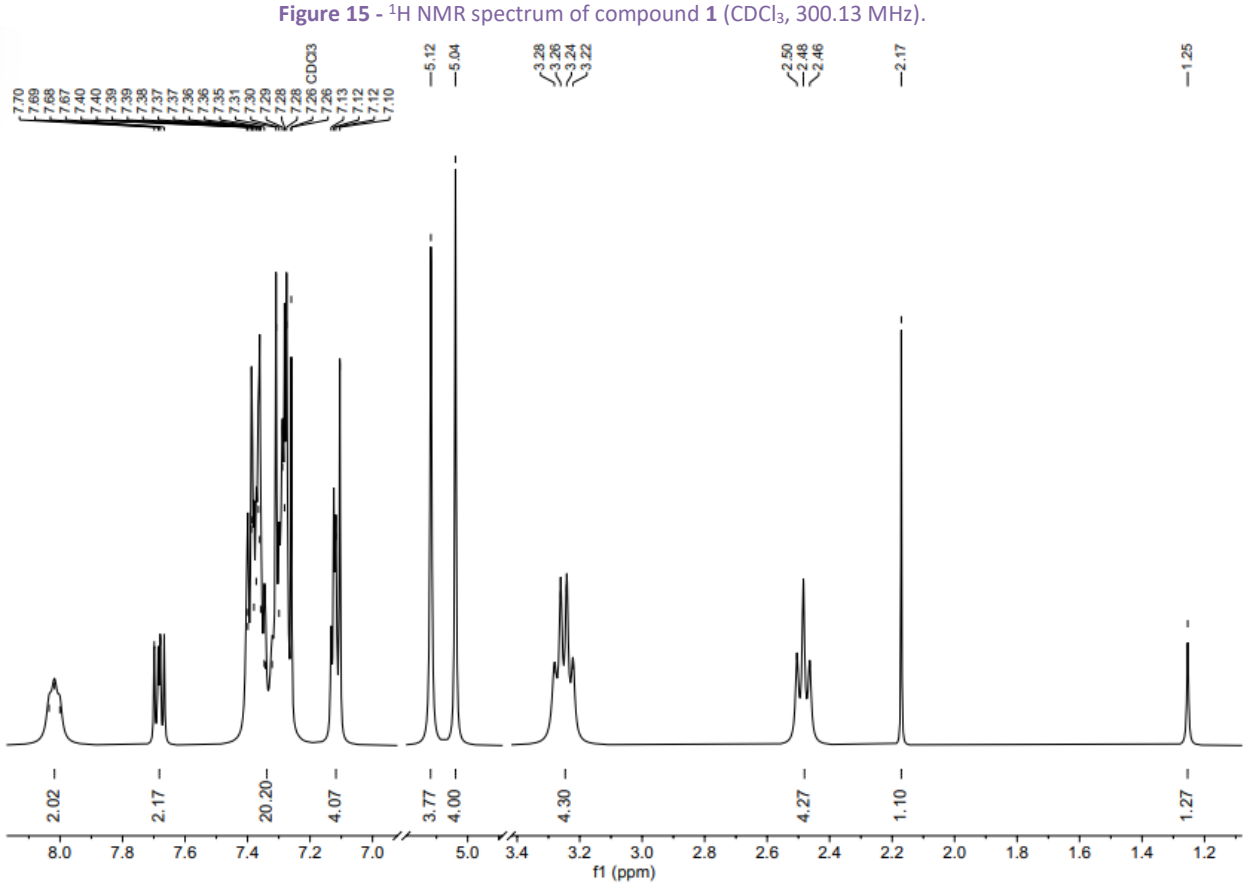

Figure 16 - ^{1}H NMR spectrum of compound **2** ($CDCl_3$, 400 MHz).

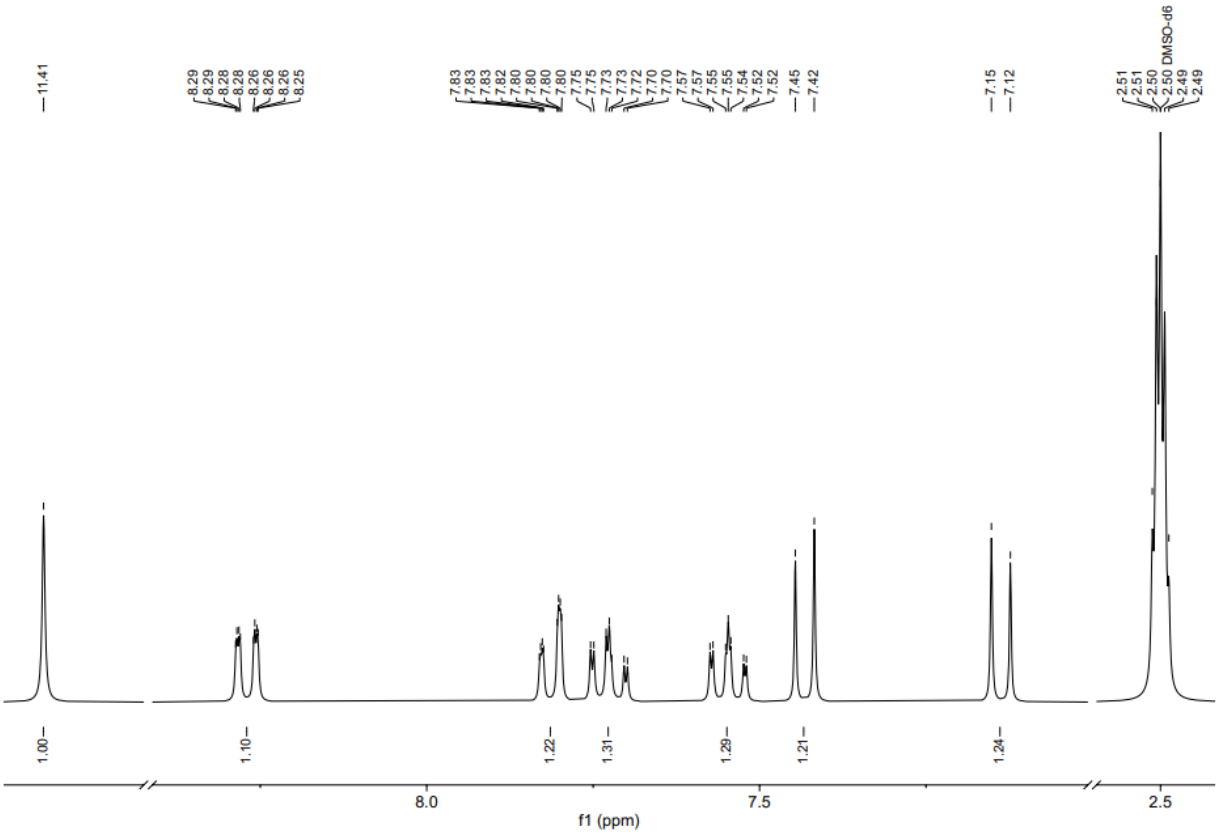

Figure 17 - ^{1}H NMR spectrum of compound **3** (DMSO-d_6, 300 MHz).

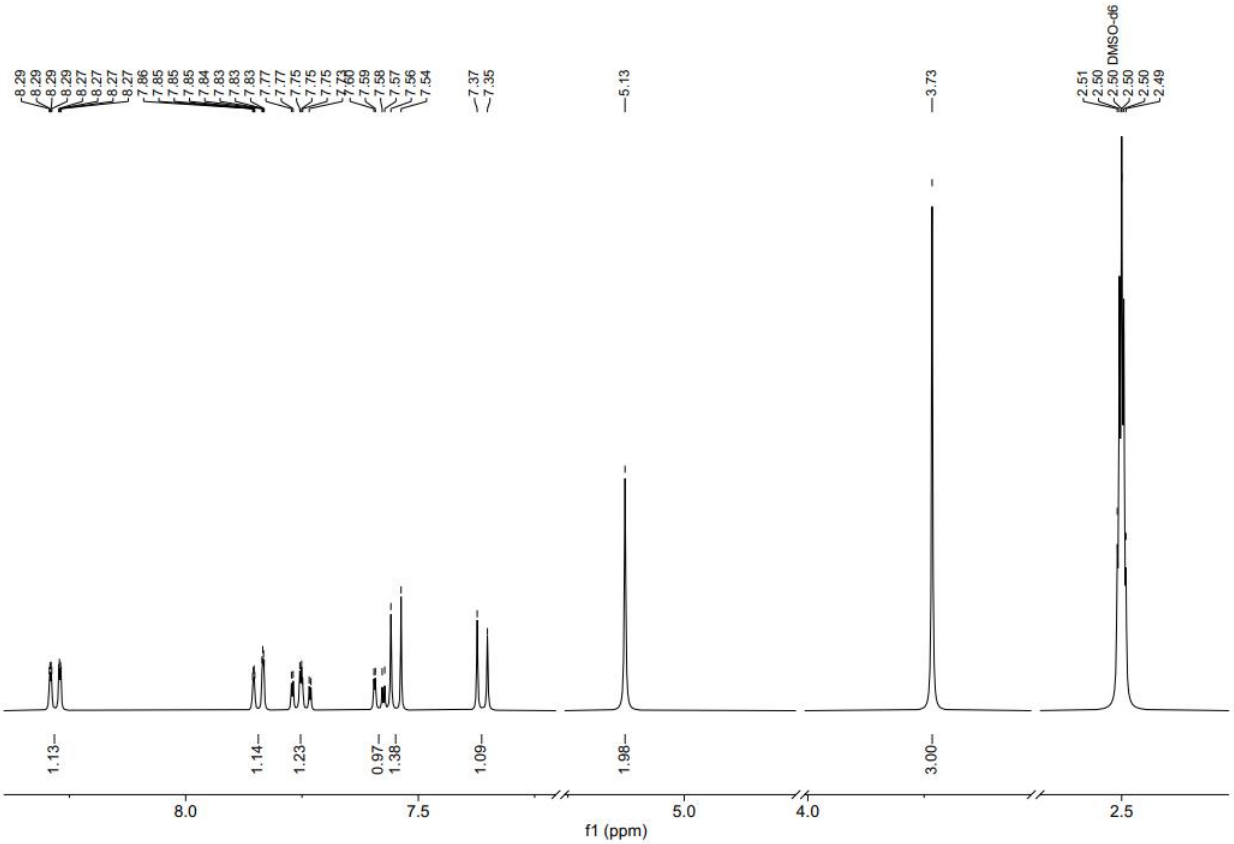

Figure 18 - ^{1}H NMR spectrum of compound **4** (DMSO-d_6, 400 MHz).

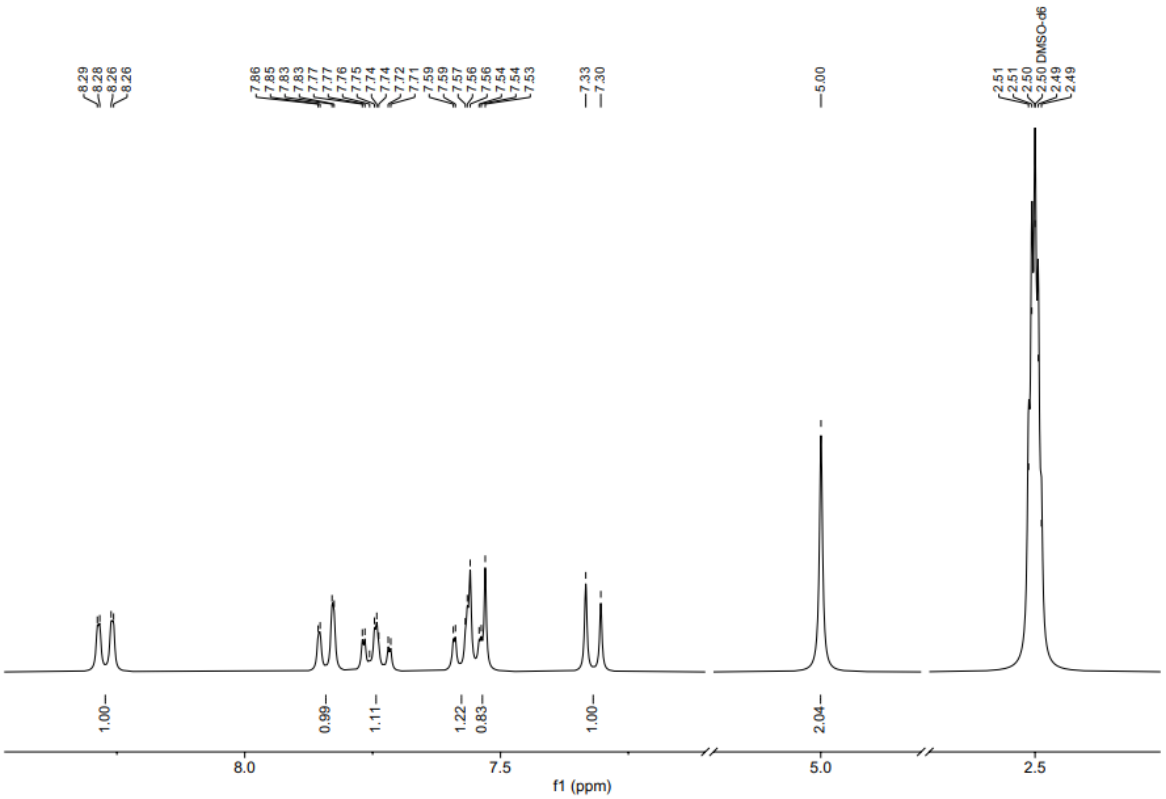

Figure 19 - ^{1}H NMR spectrum of compound **5** (DMSO-d_6, 400 MHz).

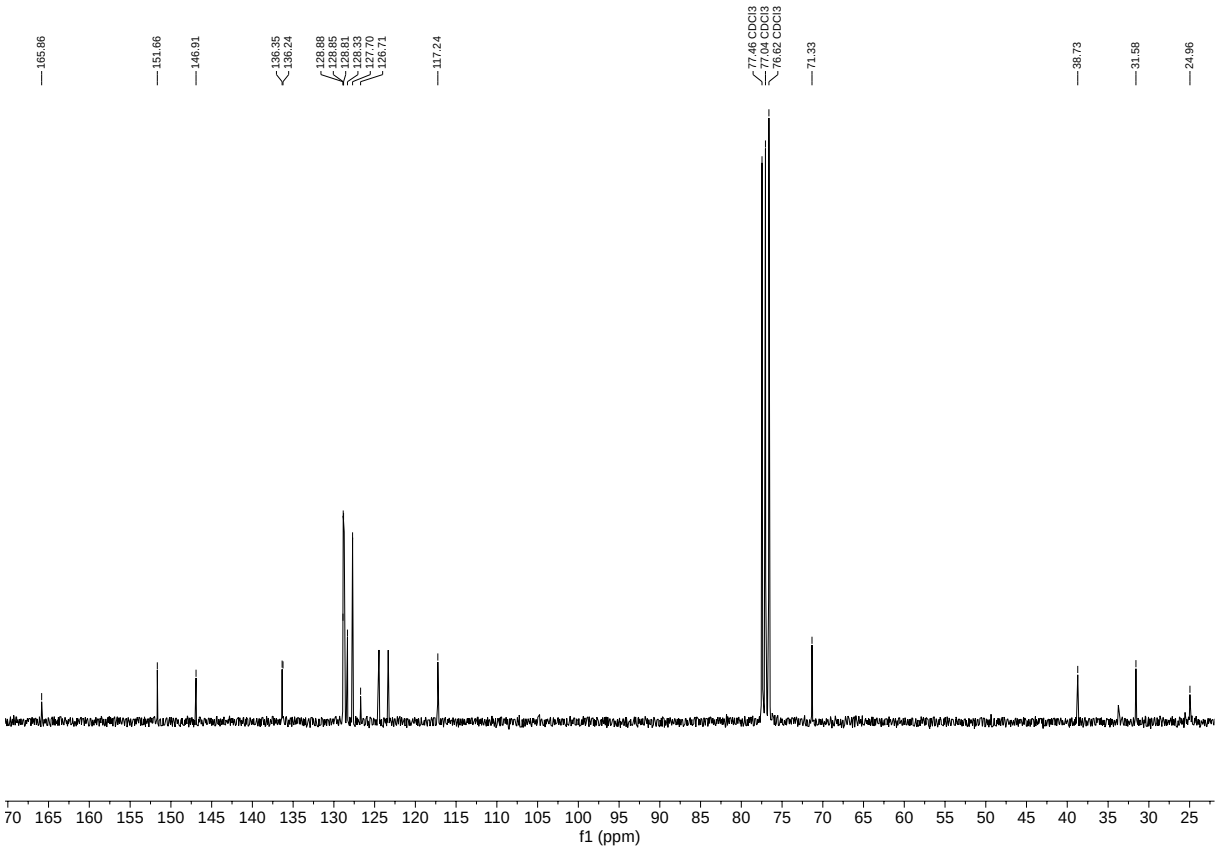

Figure 20 - ^{13}C NMR spectrum of compound **1** (CDCl3, 400 MHz).

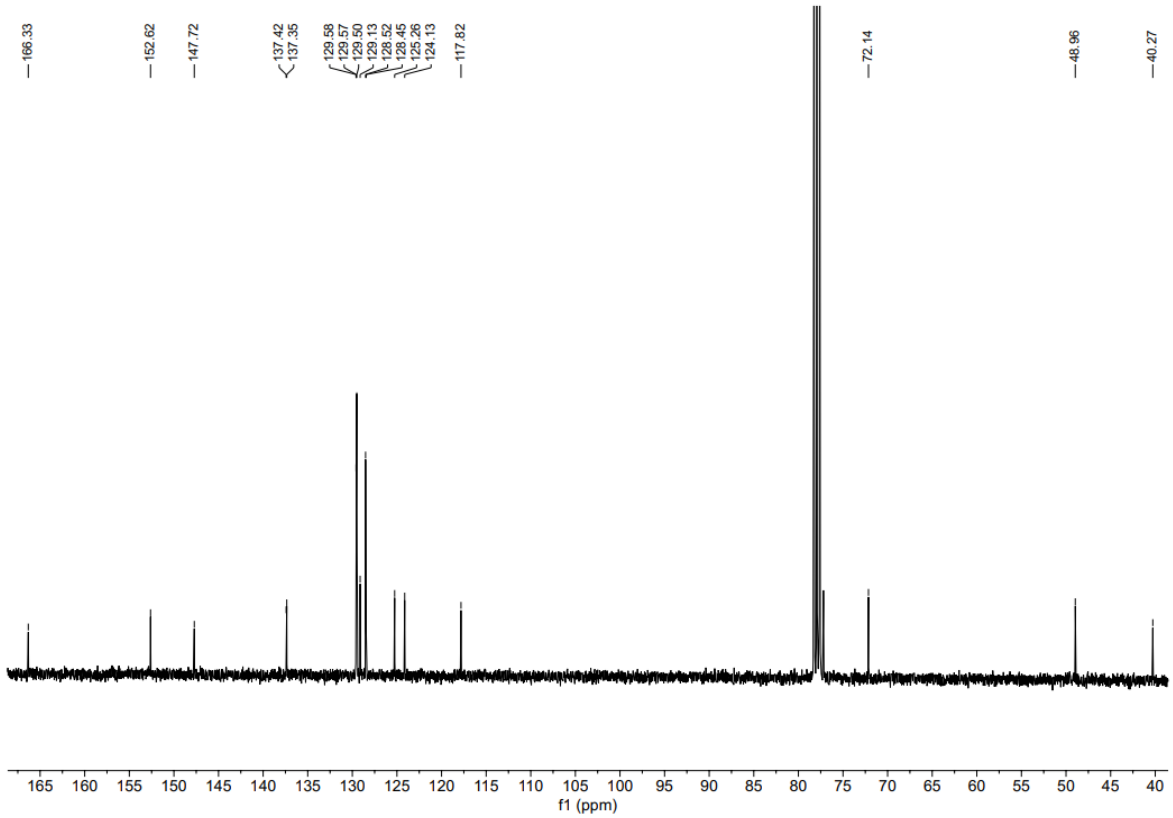

Figure 21 - ^{13}C NMR spectrum of compound **2** (CDCl3, 400 MHz).

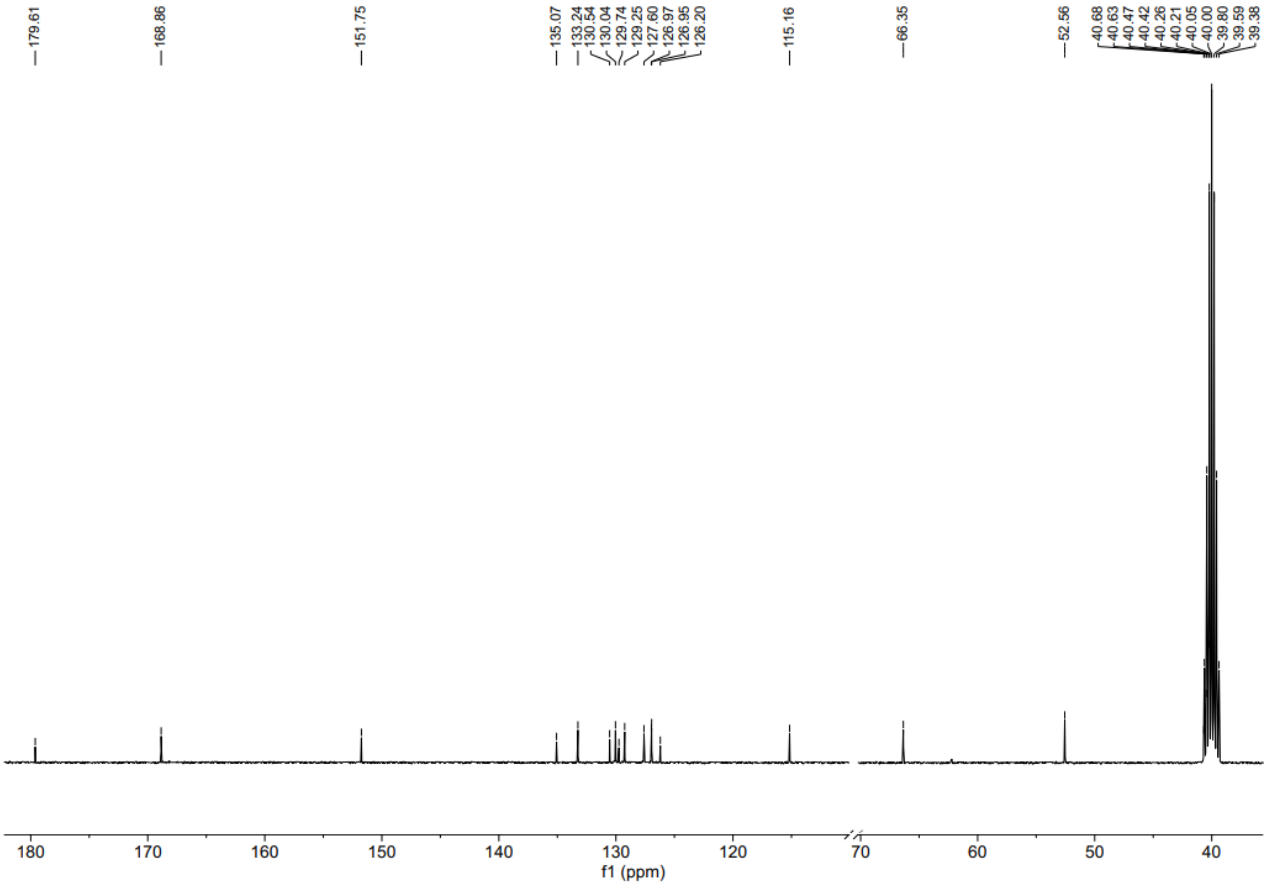

Figure 22 - ^{13}C NMR spectrum of compound **4** (DMSO-d_6, 75.45 MHz).

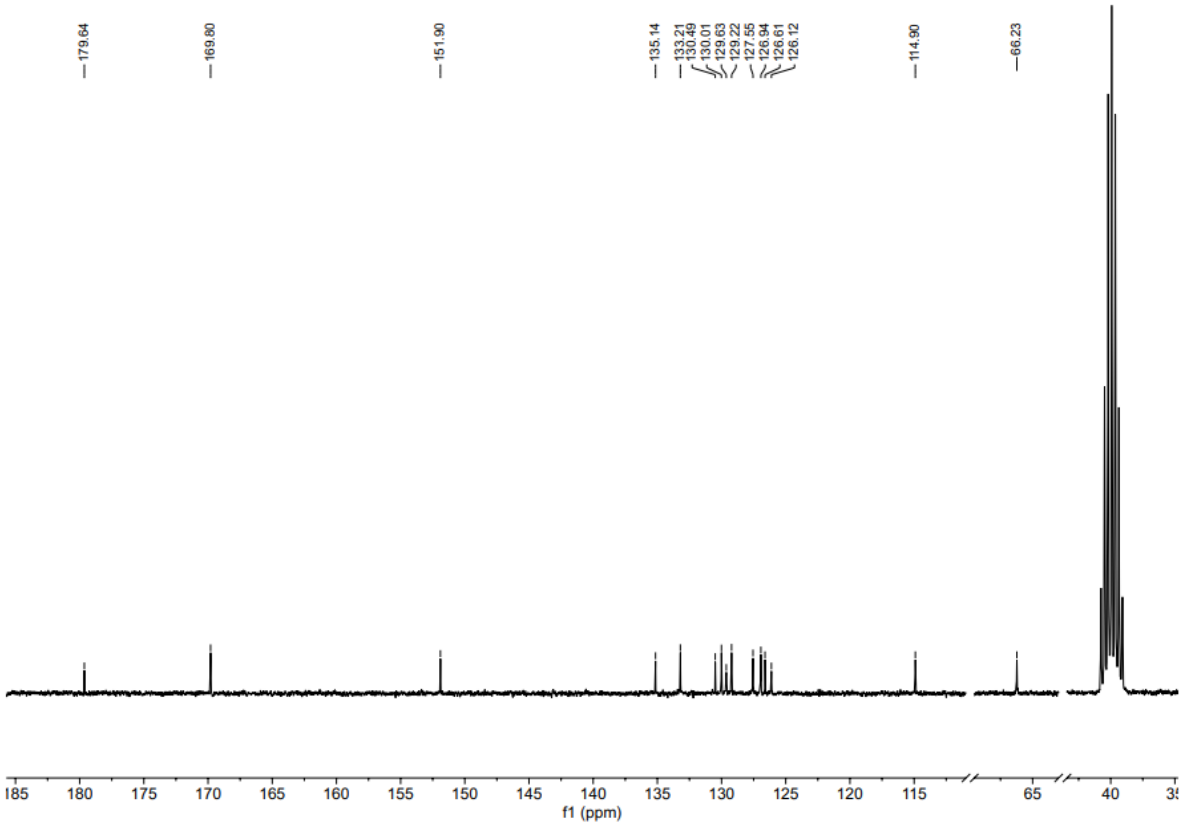

Figure 23 - ^{13}C NMR spectrum of compound **5** (DMSO-d_6, 75.45 MHz).